Unraveling the Mysteries of the Growth Plate

An approach in modeling and mapping the process of endochondral ossification without the need for animal sacrifice

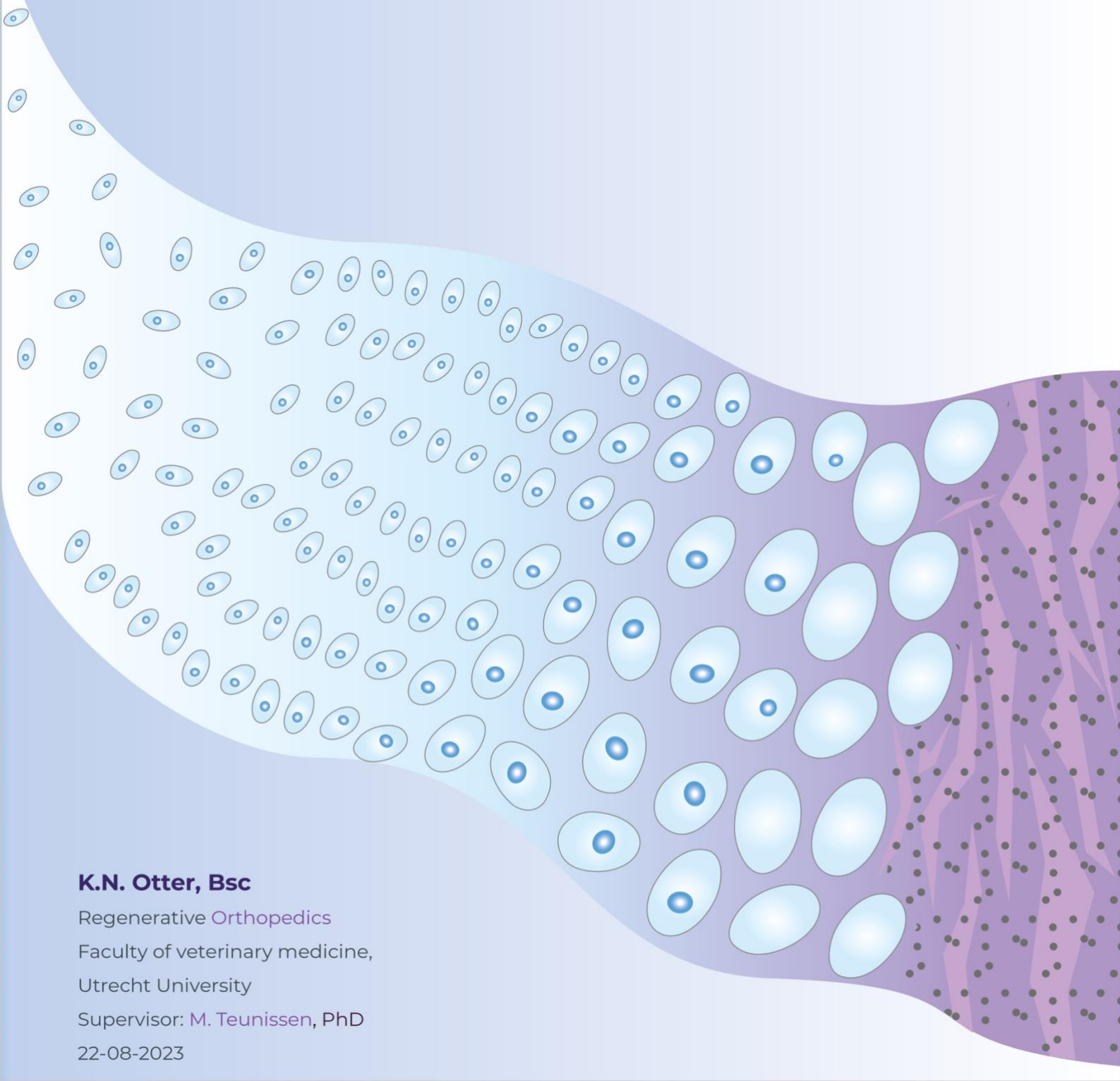

K.N. Otter, Bsc
Regenerative Orthopedics
Faculty of veterinary medicine,
Utrecht University
Supervisor: M. Teunissen, PhD
22-08-2023

This thesis is written by K.N. Otter (6715974)
Master program Regenerative Medicine and Technology
Utrecht University
Regarding the major research project component

22-08-2023

Credits go to my daily supervisor
M. Teunissen, PhD
And to the entire regenerative orthopaedics group of
Prof. M.A. Tryfonidou, DVM, PhD

Front image is created using Adobe Illustrator and formatted in Adobe InDesign by K.N. Otter

Table of contents

Abstract

The musculoskeletal system, fundamental to mobility, is reliant on the intricate organisation of the musculoskeletal tissues including bones, cartilage, tendons, and muscles. The foundation of these tissues is laid during embryonic development through two distinct mechanisms, endochondral and intramembranous ossification. The former entails the differentiation of mesenchymal stem cells into chondrocytes, forming a cartilaginous template that matures into bone. The epiphyseal growth plate, a structure at the end of long bones, regulates longitudinal bone growth through chondrocyte proliferation, differentiation, and ultimately, apoptosis or trans differentiation into osteoblasts. This process separates the growth plate in distinct zones: resting, proliferative, and hypertrophic, each with unique cellular characteristics and matrix composition.

Trauma induced large bone defects that the body itself is unable to repair highlight the need for new treatment strategies. Current strategies to treat large bone defects include grafts. However this approach encounters limitations, which shows the need to explore novel bone regeneration strategies. Studying endochondral ossification, particularly intriguing due to its hypoxia-tolerant nature, presents such a promising strategy. However, this requires a comprehensive understanding of endochondral ossification, a gap that studying the epiphyseal growth plate can help fill.

Animal models are indispensable tools used for growth plate research, even though challenges arise in direct translation of the findings in these models to humans. *In vitro* models provide controllability, allowing manipulation and large-scale analysis to study endochondral ossification more extensively. Additionally, they have the potential to replace animal models according to 3Rs principle. The ATDC5 cell line is an excellent candidate to model endochondral ossification due to its chondrogenic differentiation potential and easy accessibility and maintenance. Nonetheless, a cell line is limited. The use of primary growth plate cells from larger and more representative animals can enhance the modelling for a better translation to the human process of endochondral ossification.

This thesis outlines a comprehensive approach to investigate growth plate biology and endochondral ossification. A 3D *in vitro* growth plate model is developed using chondrogenic ATDC5 cells to simulate chondrogenic maturation. Subsequently, primary growth plate cells from dogs and pigs are isolated to elevate the model and explore surface markers for identifying resting zone progenitors. Promising markers are identified, which lays a foundation for future research in progenitor cell isolation.

Results demonstrate successful induction of chondrogenic maturation and differentiation in ATDC5 cells and establishment of a 3D model utilizing primary dog growth plate cells. Potential markers, CD146, CD105, CD90, CD44, CD73, and CD271, for identifying progenitor cells are validated for presence and expression in the resting zone. This work provides the foundation for advanced *in vitro* models, offering insights into endochondral ossification and potential applications in growth disorders, musculoskeletal diseases, and regenerative therapies. As the journey continues, these findings promise to enhance our comprehension of bone formation and contribute to improving global health and well-being.

Layman’s summary

The musculoskeletal system, which includes bones, cartilage, tendons, and muscles, is essential for our ability to move and walk. Sometimes things can go wrong, like when you break a bone. Usually, the body heals this nicely, but occasionally a permanent gap forms that the body itself can't fix. In order to repair the defects, we often need to use extra parts, like grafts, to help them heal. Right now, the most used grafts come from your own body. This not only lowers the chance of your body rejecting them, but this also means that the graft consists of all necessary components for correct healing, including blood vessels. However, a major problem is that these types of grafts are not always available. Another way is the use of grafts donated by other people; however, this can result in your body fighting the graft. Last but not least, we can also use man-made grafts, but these have trouble fitting and are hard to be recognized by your body as its own. A new idea that seems promising is to wake up your body’s ability to naturally fix bones. This is not easy and comes with its own problems like a lack of blood flow that is often missing.

But there's good news! We have a way to learn more about the process of bone healing from the body itself on how to make things better. Most of the time, when a bone breaks, it heals directly by fusing blood vessels over the break and stimulating bone cells to produce new bone tissue. Another approach involves transforming stem cells into cartilage cells first. These cells require less oxygen and don't need blood vessels. With the right signals, these cartilage cells can then transform into bone cells and create new bone.

This second process is something that actually happens naturally in the body during growth, specifically in the growth plates. The growth plates are areas of cartilage in long bones like the femur in your upper leg or the humerus in your upper arm. In these growth plates, this process ensures gradual bone growth, which contributes to the body's overall lengthening. If we can better understand this process in the growth plates, we might be able to apply that knowledge to improve treatments for large bone defects as a result of trauma or maybe a large surgery to remove a bone tumour.

Studying the growth plate up close in a model can provide us with new information on how bone formation actually happens in the human body. In this thesis I will model bone formation in the ATDC5 cell line and in primary growth plate cells in the lab. The goal is to understand the processes underlying bone elongation and identify the stem cells of the growth plate. This could shed light on potential advancements in developing regenerative strategies for stimulating the body to heal itself, ultimately improving lives of animals and humans with large bone defects worldwide.

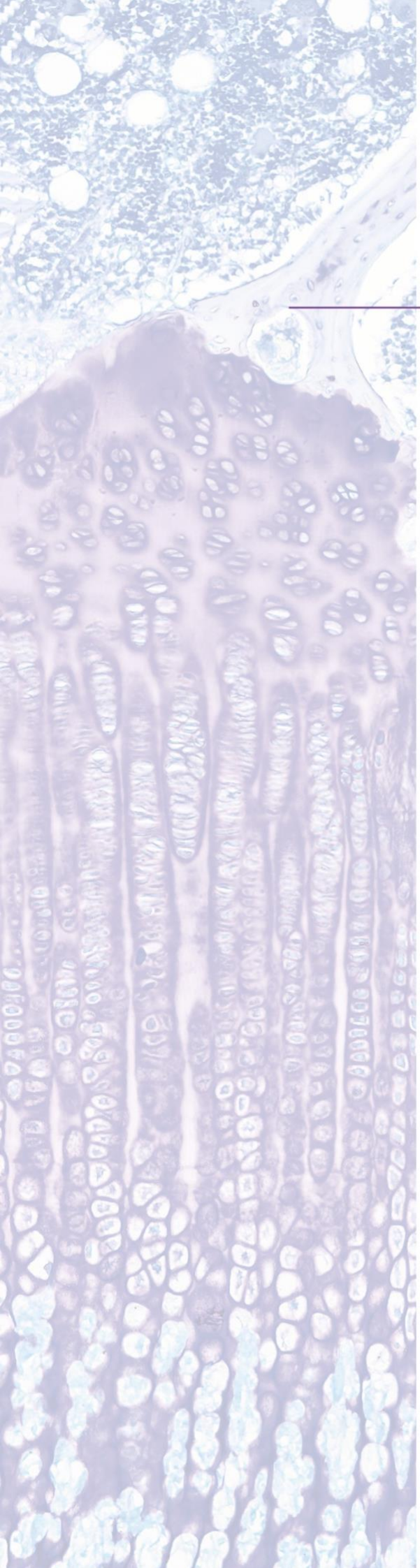

Chapter 1

General introduction

Large bone defects

The ability to move and walk around is a crucial part of our daily life. These abilities are supported by the musculoskeletal system, which includes the bones, cartilage, tendons, and muscles. Unfortunately, a fault in any of the components of the musculoskeletal system has tragic consequences on this ability, for example a fractured bone. Fractures and other bone defects can be the result of trauma, cancer, or infection. When extensive enough, the body is unable to repair these large defects itself. Several options to heal these large defects, including allografts, xenografts, and synthetic grafts, are already in use, each with its own set of restrictions [1]. At this moment, vascularized autografts are considered the gold standard for the treatment of large bone defects because of their osteoinductive and osteoconductive properties as well as a low risk of rejection. However, only a limited amount of bone is available and there is a heightened risk of infection since two surgeries are needed retrieve and to place the autograft at the site of the defect [2]. Allografts do not have these disadvantages. However, they have a higher susceptibility for immunological rejection which is likely to cause failure in the recovery and a major health risk for the patient [3,4]. A solution to overcome the abovementioned is the use of synthetic grafts. These grafts have a high safety and minimal rejection potential. Unfortunately, at this moment, they also show poor bone integration and a slow remodelling process. This can be a large burden in patient recovery [1,5,6]. A new, and in theory, a better approach would be to stimulate the body's ability to regenerate bone. However, a major setback in bone regeneration strategies at the moment is a lack of perfusion in the tissue. This often results in cell death and ultimately tissue failure before regeneration is even started. Fortunately, the body itself provides the ultimate tool to study the process of bone regeneration in a manner that does not require the tissue to be perfused. For this, a broader understanding of the process of ossification during post-natal development is essential.

The process of ossification during development

The formation of bone occurs via two different pathways, endochondral or intramembranous ossification. During intramembranous ossification mesenchymal stem cells differentiate directly into osteoblasts. This is the mechanism of bone formation for most cranial bone structures. During the second mechanism, endochondral ossification, mesenchymal stem cells differentiate into chondrocytes. These chondrocytes form a cartilaginous template which is subsequently replaced by bone. This mechanism of bone formation occurs mainly at the epiphysis and diaphysis. First, a primary ossification centre is developed in the diaphysis of the long bones (**Figure 1**). in which osteoblasts and blood vessels infiltrate and start replacing the cartilaginous template. Following the establishment of the primary ossification centre, a secondary ossification centre is formed in the epiphysis following the same path. At the end of embryonal development, the un-calcified cartilage tissue is restricted to two areas in the bone, the articular cartilage regions, and the epiphyseal growth plate [7].

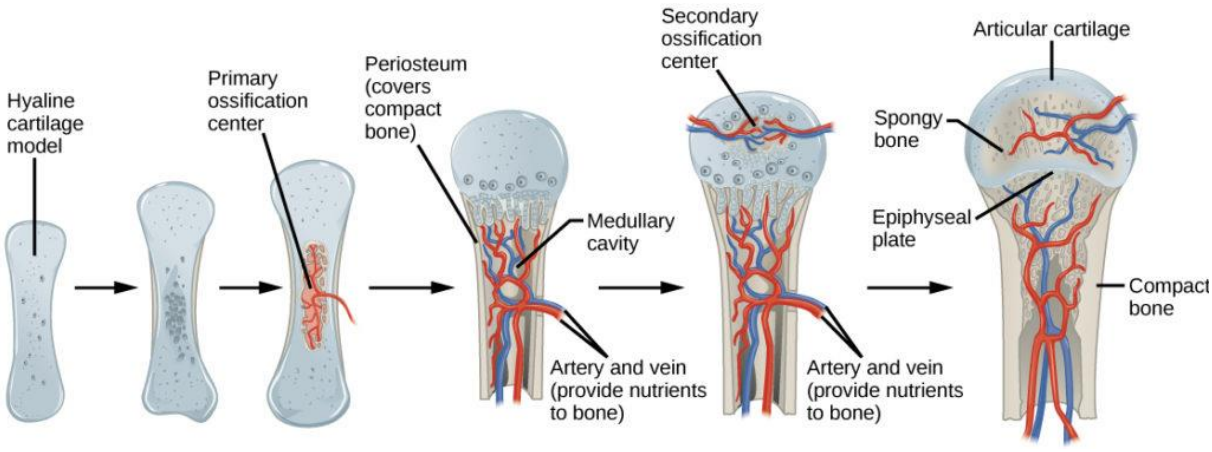

Figure 1: Overview of endochondral ossification in which the cartilage template is replaced via the formation of a primary and secondary ossification centre. Figure obtained from Thorfve, 2014 [8]

The epiphyseal growth plate is a tightly organized structure located at the distal end of the long bones. This structure is responsible for longitudinal bone growth during post-natal development and regresses when the sexual maturation is completed and the final adult height is achieved [9]. In the growth plate, chondrocytes proliferate and differentiate towards a hypertrophic phenotype. Eventually, the cells undergo apoptosis or transdifferentiate towards an osteoblastic phenotype to generate bone. The transition from cartilage to bone divides the growth plate into three distinct zones. The resting zone is located in proximity to the epiphysis and contains slowly replicating progenitor cells that replenish the growth plate. The resting zone transitions into the proliferative zone where cells start to align along the longitudinal axis and replicate more frequently. Subsequently, the transition from proliferation to terminal differentiation is marked by the hypertrophic zone. This most terminal part of the hypertrophic zone is invaded by blood vessels originating from the metaphyseal bone. Invasion of osteoblasts and osteoclasts via these blood vessels results in the remodelling of the hypertrophic cartilage into calcified bone structures [9,10].

Morphology and physiology of the growth plate chondrocytes

The zones defined in the epiphysial growth plate each have their own cellular and structural composition due to tight regulation in the process of chondrogenesis and endochondral bone formation (**Figure 2**). In the resting phase, chondrocytes appear relatively inactive in terms of proliferation and matrix production and are labelled as the stem cells of the growth plate. Cellular morphology is characterized by small, compact, and uniform cells that appear single or in pairs. *COL2A1* is highly expressed in the resting chondrocytes, leading to a collagen type II-rich matrix surrounding the cells. Characteristic of the resting zone is that the matrix takes up more space compared to the chondrocytes. During the proliferating phase, the chondrocytes start becoming more active and start secreting more matrix rich in collagen type II and glycosaminoglycans (GAGs). Proliferating chondrocytes have a flat phenotype and occur in longitudinal columns. After rapid proliferation, cells start to differentiate into a hypertrophic phenotype and start to secrete collagen type X, while reducing the collagen type II secretion gradually. The cell vacuoles increase ten times in size and DNA synthesis decreases while matrix production is largely upregulated. In the final stages of differentiation, the cells stop producing collagen and matrix altogether and enter a terminal phase right before the remodelling into bone [11,12]. The differences in cellular morphology and matrix deposition allow for a clear histological distinction between the zones in the growth plate.

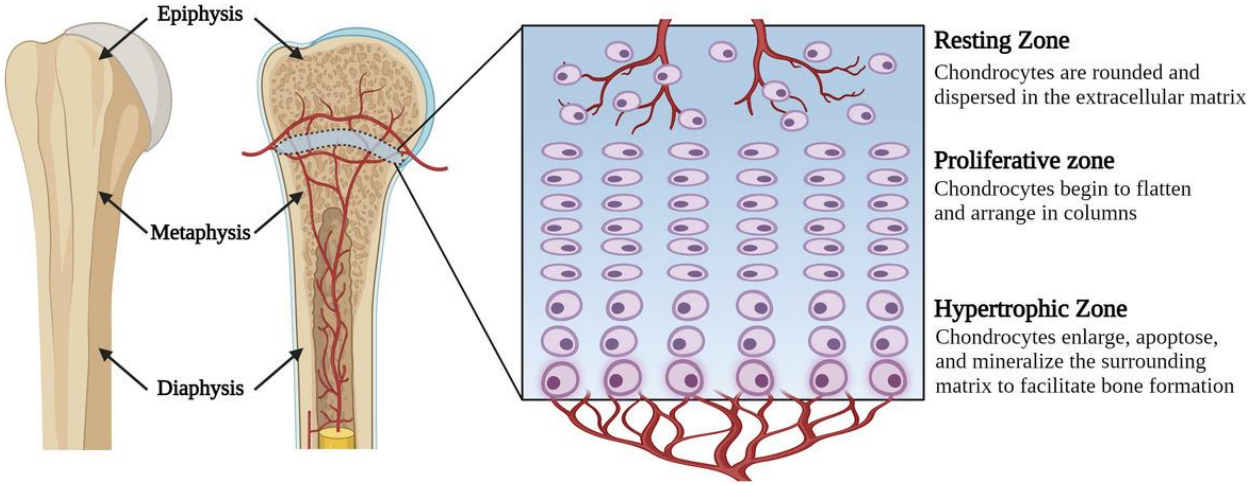

Figure 2: a schematic overview of the localisation of the growth plate in the long bones and the different stages of chondrogenic maturation in the growth plate. This displays the difference in morphology between the different zones in the growth plate. Figure obtained from Tiffany et al, 2022 [13]

Spatial regulation in the epiphysial growth plate

The process of endochondral ossification is tightly regulated by a complex array of signalling molecules incorporated in pathways that guide proliferation, differentiation, matrix production, apoptosis, and vascular and bone cell invasion (**Figure 3**). The signalling molecules regulating these complex processes include Indian hedgehog (IHH) and parathyroid hormone-related protein (PTHrP), bone morphogenetic proteins (BMPs), WNT and other growth factors like fibroblast growth factors (FGF). On top of that, the rate of endochondral ossification is mainly regulated by endocrine signalling molecules which consist of several hormones like androgens and estrogens [10]. A broad understanding of the explicit processes regulating endochondral osteogenesis can be beneficial to a variety of causes, including increasing the knowledge behind differences in adult height, with the possibility to explain underlying causes of growth disorders, acquiring insight into the process underlying osteoarthritis, and achieving new insights into bone regeneration potentials.

The Indian hedgehog/parathyroid hormone-related protein pathway is a key regulator during endochondral ossification. IHH is a paracrine regulator in the development of bone and mainly influences the proliferation and differentiation of chondrocytes in the early zones of the epiphysial growth plate. The factor is expressed by hypertrophic chondrocytes and diffuses towards the resting zone where it binds to its receptor, PATCHED-1. The activation of PATCHED-1 results in downstream signalling via SMOOTHENED (Smo) and transcription factors of the Gli family which leads to an elevation in the expression of PTHrP by the periarticular chondrocytes located at the far distal end of the long bones. The PTHrP protein diffuses through the growth plate which creates an expression gradient causing a delay in the differentiation of proliferating chondrocytes towards the hypertrophic phenotype. This increases the distance between the IHH-expressing hypertrophic chondrocytes and the *PATCHED-1*-expressing resting zone chondrocytes, creating a negative feedback loop that mainly controls the foetal growth plate development. The negative IHH/PTHrP feedback loop is extremely important in maintaining the growth plate during post-natal development as well. Inactivation of one of the factors leads to abrupt fusion of the epiphysial growth plate suggesting the importance of the pathway in the growth of long bones until final adult height is reached [14,15].

Bone morphogenetic proteins (BMPs) are growth and differentiation factors that are essential during various stages of endochondral ossification and angiogenesis. BMPs belong to the TGF-β superfamily of paracrine factors and act through serine-threonine kinase receptors. Activation of these receptors leads to a cascade reaction in which SMAD proteins are activated through phosphorylation [16]. A BMP gradient is formed along the growth plate by the expression of BMP antagonists mainly in the resting and proliferative zone, while BMP ligands are mainly expressed by chondrocytes in the hypertrophic zone [17,18]. A study by Garrison *et al*, 2017 revealed that BMP-2, BMP-4 and BMP-6 are BMP agonists which are mainly expressed in the hypertrophic zone and that BMP-3 and GREM1 which are BMP antagonists are highly expressed in the resting zone [16]. The BMP gradient in the growth plate initializes differentiation toward a hypertrophic phenotype and is a trigger for apoptosis in the terminal growth plate while maintaining the undifferentiated proliferating zone via the distribution of BMP antagonists [16,19]. In total, 14 different BMPs have been identified of which BMP-2, 4, 5, 6, 7, and 9 exhibit high osteogenic activity. These BMPs are also active during endochondral bone development in which BMPs act by maintaining *SOX9* expression. This transcription factor is important in chondrogenic commitment and steers differentiation of chondrocytes. BMP-4 has a specific important role in the processes of osteoblastogenesis but also has a regulating function in chondrocyte proliferation, differentiation, and apoptosis during endochondral ossification [20,21]. BMP function relies heavily on the expression of TGF-β to maintain a homeostatic environment during chondrogenesis and endochondral ossification. TGF-β signalling causes a cascade reaction in which BMP-SMAD signalling is suppressed. This ultimately represses the hypertrophic maturation of chondrocytes. The production of TGF-β is thus a gatekeeper in the prevention of early maturation of chondrocytes in the resting and proliferating zone of the growth plate [22].

SOX9 has also proven to be a major factor in directing hypertrophic maturation of the growth plate chondrocytes and in preventing further differentiation to an osteoblast phenotype. The BMP/TGF-β pathway is essential in maintaining *SOX9* expression [23]. The *SOX9* gene is active very early during development and is essential in guiding precursor cells towards a chondrogenic lineage, but remains highly expressed during post-foetal development throughout the growth plate [24]. SOX9 is proven to maintain columnar proliferation in the proliferative zone and thereby delay pre-hypertrophy and prevent osteoblastic dedifferentiation by lowering β-catenin signalling and *RUNX2* expression. Contrary to that, SOX9 expression is also essential for inducing hypertrophy of the chondrocytes due to its binding to the *COL10A1* promotor in hypertrophic cells which induces upregulation of *COL10A1* expression [24–26].

Another important factor in growth plate regulation is NOTCH. This is one of the most evolutionary conserved genes and it is heavily involved in cell fate determination, differentiation, proliferation, and apoptosis. *NOTCH* acts upstream of *SOX9* and *RUNX2*, two major transcription factors in growth plate regulation. For example, *NOTCH* negatively regulates chondrocyte differentiation by suppressing *SOX9* expression. Since NOTCH has such a broad range in development, it is hard to pinpoint the exact influence on growth plate regulation, however, a NOTCH knockout results in several skeletal malformations, highlighting the important role NOTCH has [23,27].

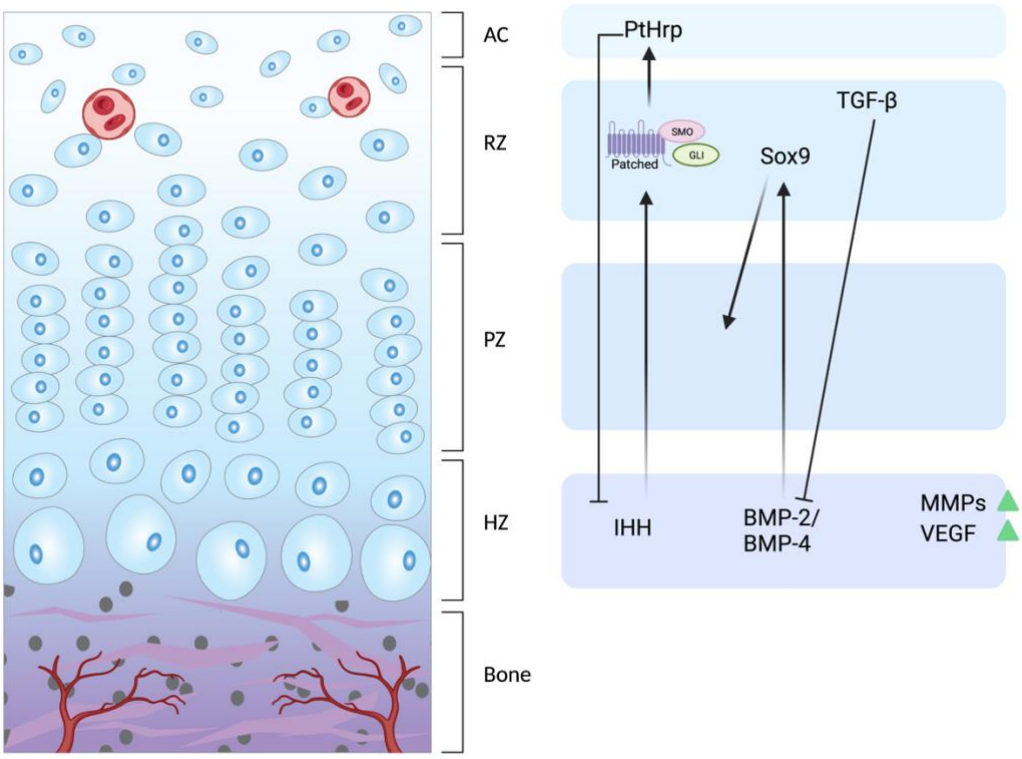

Figure 3: a schematic overview of the regulation in the growth plate. Arrows indicate activation, and lines indicate inhibition. Created with BioRender

The precise regulation of the growth plate is an intricate process characterized by significant gaps in our current knowledge. A more comprehensive understanding of spatial regulation can be of tremendous help in discovering underlying mechanisms of growth anomalies, while simultaneously providing novel insights for the development of new regenerative strategies targeting bone and cartilage.

Animal models

Currently, growth plate biology is often studied using animal models. However, the use of animal models has several advantages and disadvantages. The advantage of using an in vivo animal model is that it allows for a testing environment consisting of a whole physiological system which can get relatively close to humans. Currently, most animal studies conducted on endochondral ossification are performed using rodent models [28]. However, the growth plate in rodents poorly represents the human situation, as the growth plate does not close upon maturation [29]. This does happen during puberty in humans. Larger animals like dogs and pigs provide a better model since growth plate closure does occur during puberty in these animals [30,31]. However, even in larger animal models, Only rarely it occurs that an experiment performed in an animal model achieves a similar result when repeated in humans [32]. In addition, according to the 3R principles, replacing animal models with *in vitro* modelling limits the need for animal sacrifice and suffering for research purposes tremendously [33].

Growth plate modelling

Growth plate modelling can also be done *in vitro.* A lot of work has already been conducted using 3D pellet culture systems using mesenchymal stem cells (MSCs) or chondrocytes directly. The models are often sufficient in studying chondrogenesis and chondrogenic maturation [13]. However, at this moment, the models are unable to show the later stages of chondrogenesis that *in vivo* results in bone elongation [34,35]. Other disadvantages include necrosis in the centre of the pellets with time and a lack of matrix deposition and cellular organization compared to the *in vivo* situation [13,36]. However, *in vitro* modelling of the growth plate has major advantages as well. 3D culture systems provide a controllable environment in which chondrogenic maturation can be steered and manipulated in an easy manner. On top of that, these culture systems allow for a variety of analysis methods including histology, fluorescent microscopy, and quantitative polymerase chain reaction (qPCR). The wide possibilities of analysis allow for extensive screening of what is happening during chondrogenic maturation. Developing an *in vitro* model of the growth plate allows studying the process of endochondral bone formation in a controllable environment. An advantage of this controllable environment is that the model is easy to manipulate and allows for more large-scale experiments. Unlike animal models, which are available in a limited manner. Furthermore, *in vitro* modelling could allow for the use of human cells as well, which overcomes several hurdles in the translatability of animal models [37].

Aims and outline of this thesis

This thesis aims to develop a three-dimensional *in vitro* model of the growth plate. The 3D culture model is designed to simulate chondrogenic maturation to obtain an easy-to-access and representative model of endochondral bone formation. Furthermore, stem cell biology is utilized in an approach to identify the growth plate progenitor cell niche located in the resting zone.

The first part of this thesis focuses on developing a 3D *in vitro* model of the epiphyseal growth plate. The aim of the study performed in **Chapter 2** is to develop a 3D spheroid culture using the mouse chondrogenic ATDC5 cell line, showing *in vivo* characteristics of chondrogenic maturation over time. The *in vitro* culture model is developed to allow a more accessible environment to study the process of endochondral ossification.

The second part of the thesis focuses on the identification and isolation of primary growth plate cells from both canine and porcine origin. These cells will be used to validate if similar results can be achieved using primary cells originating from the growth plate in the *in vitro* model established in **Chapter 2**. This would allow the *in vitro* model to be utilized with specific cells allowing more extensive screening of the process of endochondral ossification. Furthermore, these cells are also used to identify a surface marker subset, specifically for identifying resting zone progenitor cells. Determining such a marker subset allows for specific cell sorting of the resting zone progenitors which would be an exciting step for future research. The sorted progenitor population could be utilized as a cell source in the *in vitro* culture model established in **chapter** 2 which allows for a more representative model of endochondral ossification *in vitro*. In **Chapter 3** expression of several promising markers will be validated in the resting zone using immunohistochemical staining and zone-specific relative gene expression analysis.

All knowledge obtained in this thesis will be summarized and discussed in **Chapter 4.** In this chapter, all results will be discussed in proximity to relevant literature and future perspectives in order to get closer to unravelling the mysteries behind the epiphyseal growth plate.

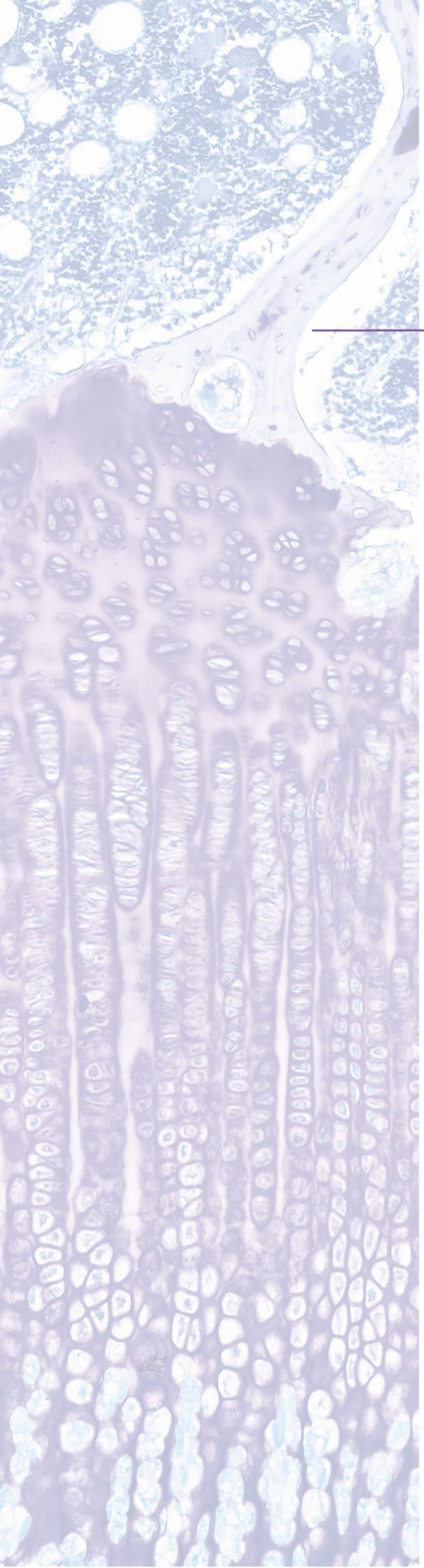

Chapter 2

Three-dimensional In Vitro Culture Model of the Growth Plate Utilizing the ATDC5 Cell Line: Simulating Endochondral Bone Formation

2.1: Introduction

The epiphyseal growth plate is a tightly regulated structure located at the distal ends of long bones during development [9,38]. The growth plate can be divided into three zones: the resting, proliferative and hypertrophic zone, each containing chondrocytes in different stages of maturation. Unravelling the precise regulation mechanisms behind endochondral ossification remains a challenge of the present. However, understanding these mechanisms could provide new insight into growth plate defects and in possible new strategies in bone and cartilage regeneration. In current research, animals are commonly utilized as models to explore these pathways. Nonetheless, animal models come with several limitations. For example, studies conducted in animals rarely result in the same outcome in humans, since no species responds the same [32]. Furthermore, growth plate morphology differs greatly between different species and animal models do not allow for large scale screening. An alternative way to minimize animal sacrifice for research purposes according to the 3Rs principle, is the utilization of an *in vitro* model [33]. An *in vitro* model provides a controllable environment that would present a suitable alternative for animal models [39,40 41].

In vitro cell culture is a frequently used method to understand mechanisms underlying cell behaviour like differentiation, growth, and mechanics *in vivo.* For more than a hundred years, two-dimensional (2D) cell cultures have been the golden standard for *in vitro* modelling to study cellular responses to induced stimulation. Although this technique has significantly improved our understanding of cellular behaviour, the 2D culture system comes with significant limitations regarding modelling the *in vivo* response. Cells *in vivo* rely on their micro-environment consisting of cell-cell interactions and cell-matrix interactions for fundamental cellular behaviour in response to the function of whole organs [42]. To overcome these limitations, culture conditions have evolved toward three-dimensional (3D) culture methods in the form of micro-aggregates, spheroids, or organoids [43]. A well-designed micro-environment can be used to stimulate extracellular matrix (ECM) production, proliferation, and stem cell differentiation in a manner closer to the *in vivo* situation compared to 2D culture [43,44].

The study conducted in this chapter will focus on the development of a 3D *in vitro* model of the epiphyseal growth plate to simulate the process of endochondral ossification. The main goal of the study is to create an easy-to-access and reproducible model to investigate the process of endochondral bone formation in the epiphyseal growth plate. This study utilizes the mouse chondrogenic ATDC5 cell line derived from mouse teratocarcinoma cells to develop a 3D spheroid model to ensure that the model is as consistent as feasible [45]. Several studies have already tried to create an *in vitro* model for endochondral ossification with the ATDC5 cell line [25,46–49]. In these studies, initial stages of chondrogenic maturation have been reached as a result of TGF-β stimulation which is characterized by chondrogenic gene expression and a GAG and collagen type II rich matrix [46,50].

The main study objective of chapter 1 is to simulate chondrogenic maturation as seen in the different zones of the growth plate over time as a response to different stimuli utilizing a 3D ATDC5 cell line culture system. I hypothesize to reach this objective via the use of different culture conditions, the addition of TGF-β and/or BMP-4 in different concentrations, and different spheroid sizes. TGF-β is added with the goal to drive matrix production and stimulate proliferation to simulate the first stages of chondrogenic maturation [21,25,46–49]. BMP-4 is known to drive chondrogenic differentiation in the growth plate and is thus added to drive chondrogenic hypertrophy and collagen X production to achieve the final stage in chondrogenic maturation [51,52]. Outcomes are measured using histology, GAG/DNA analysis and RT-qPCR to validate matrix disposition and gene expression as a method to validate chondrogenic maturation.

2.2: Materials and methods

Cell culture
ATDC5, a mouse chondrocyte precursor cell line retrieved from mouse teratocarcinoma cells was provided by RIKEN cell bank [45]. The ATDC5 cells were expanded in advanced DMEM-F12 (Gibco, 11540446) media supplemented with 5% foetal bovine serum (Biowest) and 1% penicillin/streptomycin (P/S; GE Healthcare Life Sciences) in an incubator at 37 C° at 5% CO_2 and around 20% O_2. Media was changed twice a week and cells are passed every 7 days when a confluence of ~90% is reached.

Spheroid 3D culture with the ATDC5 cell line
Subconfluent ATDC5 cells were released from a T75 flask using TripLE™ Express Enzyme (1X, Gibco, 12604013), centrifuged at 500*g* for 5 minutes and resuspended in DMEM-F12 medium containing 1% P/S. Spheroids were formed by seeding 35.000 or 100.000 cells in an ultra-low attachment U-bottom 96 well plate (Costar, 28022057) in 100 µL or 200 µL chondrogenic differentiation medium (**Table 1**) respectively. The spheroids self-assemble within 24 hours. The medium was refreshed every 2-3 days and the spheroids are collected at set time points.

Culture conditions ATDC5 spheroid culture optimisation
In the first culture condition optimisation experiment three different media compositions, two culture conditions and two spheroid sizes were compared. The chondrogenic normal differentiation medium (NM) consisted of DMEM-F12 medium supplemented with 1% P/S and 2% ITS+ premix (Corning™, 354352). The insulin likely slows down proliferation and enhances matrix production. Advanced chondrogenic differentiation medium (AM) consisted of the NM medium supplemented with additional proline (40µg/mL, Sigma-Aldrich, 147853) to provide the correct building blocks for collagen II synthesis, L-ascorbic acid 2-phosphate (0.2 mM, Sigma-Aldrich, 1713265258) to prevent deficiency resulting in poor proliferation and matrix production [53], dexamethasone (200 nM, Sigma-Aldrich, 50022) which provides glucocorticoids (GCs)[54,55], and TGF-β (5 ng/mL, R&D Systems, 240-B). Media composition is based on previous literature on chondrogenic maturation [47,56–59]. The third media condition is the AM medium supplemented with 5% FBS (Biowest) (AM+) for extra nutrient addition. The cells are incubated at 37 C° with 5% CO_2 and around 20% O_2 under normoxic culture conditions, or at 37 C° with 5% CO_2 and 5% O_2 under hypoxic culture conditions. In this experiment, spheroids were cultured for a total period of 14 days.

As this did not result in the desired results, a follow-up experiment was performed in which the addition of TGF-β (5 ng/mL and 50 ng/mL, R&D Systems) was compared to the addition of BMP-4 (50 ng/mL, Gibco, PHC9533) during 21 days or TGF-β (5 ng/mL) for the first week followed by BMP-4 (20 ng/mL) for the remaining two weeks. In this optimisation, spheroids are formed according to the same protocol mentioned above, except all spheroids consisted of 35.000 cells, were cultured under normoxic conditions (37 C°, 5% CO_2, and 20% O_2), and were cultured for a total period of 21 days.

Spheroids were collected at set time points on day 1, day 7, day 14 and day 21 of culturing and were collected for histology, immunohistochemical evaluation, glycosaminoglycan (GAG), and DNA analysis, and reverse transcription-quantitative polymerase chain reaction (RT-qPCR) (N=2).

Normal diff. medium (NM)	Advanced diff. medium (AM)	Advanced diff. medium + (AM+)
DMEM/F12	DMEM/F12	DMEM/F12
ITS+ premix (2%)	ITS+ premix (2%)	ITS+ premix (2%)
Penicillin/streptomycin (1%)	Penicillin/streptomycin (1%)	Penicillin/streptomycin (1%)
	Proline (40 µg/mL)	Proline (40 µg/mL)
	L-ascorbic acid 2 phosphate (0,1 mM)	L-ascorbic acid 2-phosphate (0,1 mM)
	Dexamethasone (100 nM)	Dexamethasone (100 nM)
	TGF-β (5 ng/mL)	TGF-β (5 ng/mL)
		FBS (5%)

Table 1: Media compositions ATDC5 spheroid and micro-aggregate 3D culture for optimization

Histological and immunohistochemical staining to characterize matrix deposition

Two spheroids per condition are fixed overnight in 4% paraformaldehyde with 1% Eosin (Merck, 115935) dissolved in PBS directly after retrieval at each time point. After fixation, to avoid loss, the spheroids were incorporated in 3% agarose. Samples were dehydrated using a sequential ethanol series in a tissue processor after three days of fixation maximum, ending in paraffin in which the samples are embedded. 5 µm sections were cut using a microtome. Before staining, sections were rehydrated using xylene followed by a graded ethanol series (100%, 96%, 70%). Glycosaminoglycans were visualized with a toluidine blue staining. Sections were stained for 10 minutes in 0,04% toluidin blue (Sigma Aldrich, T3260-5G) in 0,2M acetate buffer, rinsed in tap water for 1 minute and dried at 40 °C. Safranin-O/Fast Green staining was performed by subjecting sections to filtered Mayers haematoxylin solution for 20 seconds and rinsing in running tap water for 10 minutes. Sections were counterstained with 0,4% aqueous Fast Green (Sigma-Aldrich, F7252-25G) for 4 minutes, rinsed twice for 3 minutes in 1% acetic acid and stained with 0,125% aqueous Safranin-O (Sigma-Aldrich, S8884-25G). After staining, sections were dehydrated using a gradual ethanol series (70%, 96%, 100%) ending in xylene (Klinipath, 4055-9005) before mounting the slides with permanent mounting medium (Sigma-Aldrich, 102506567.

Immunohistochemical evaluation for collagen type I, type II, and type X was performed. Sections were rehydrated, washed with 0,1% PBS-Tween (Boom, 76021765) and blocked with 0,3% H_2O_2-PBS for 10 minutes. For collagen I and collagen II, antigen retrieval consisted of 1 mg/mL pronase (Roche, 11459643001) in PBS for 30 minutes at 37 °C followed by 10 mg/mL hyaluronidase (Sigma-Aldrich, H3506) in PBS for 30 minutes at 37 °C. To limit non-specific binding, sections were blocked with 5% BSA in PBS for 30 minutes before overnight incubation at 4 °C with anti-collagen I primary mouse monoclonal antibody (Abcam, Ab6308) or with anti-col2a1 mouse monoclonal antibody (DSHB, II-II6B3). Antigen retrieval for collagen X consisted of 0,1% pepsin (Sigma-Aldrich, P7000) in PBS for 20 minutes at 37 °C followed by 10 mg/mL hyaluronidase (Sigma-Aldrich, H3506) in PBS for 30 minutes at 37 C°. These samples were blocked with 0,3% H2O2-PBS for 10 minutes followed by a 1:10 normal goat serum-PBS block for 15-30 minutes before overnight incubation at 4 C° with anti-collagen X mouse monoclonal antibody (Quartett, 2031501005). Normal mouse IgG1 (Dako, X0931) in corresponding concentrations was used as a negative isotype control for all three immunohistochemical stainings. After washing with PBS, slides were incubated for 30 minutes at RT with BrightVision Poly HRP anti-Mouse IgG secondary antibody (Immunologic, VWRKDPVM110HRP). Brown staining was developed by incubating sections with Bright-DAB Substrate Kit (Immunologic, BS04-110) for a maximum of 5 minutes or until brown staining was visibly developed. Sections were rinsed with milliQ and demi water respectively and counterstained with filtered Mayers

haematoxylin for 30 seconds (Sigma Aldrich, MHS32-1L) and dehydrated following the method mentioned before. Histological sections were analysed using light microscopy (Olympus BX51).

DNA and GAG content analysis

Two pellets per condition were pooled together and digested overnight in papain digestion solution consisting of 10 mM Papain (Sigma-Aldrich, P3125), 10 mM Cysteine HCL (Sigma-Aldrich, C9768-5G), 200 mM H_2NaPO_4*2 H_2O (Boom, 21254), and 10 mM EDTA (Merck Millipore, 100944) at 60 C°. The DNA content of the micro-aggregates was measured using the Qubit dsDNA High Sensitivity Kit (Invitrogen, Q32851) according to the instructions from the manufacturer. To quantify the GAG content in the micro-aggregates, a dimethyl methylene blue (DMMB) assay was performed with the papain digested samples. After the addition of DMMB solution, the absorbance was immediately measured (540/595 nm) using a microplate multimode plate reader (VANTAstar, BMG Labtech). The GAG content was validated based on a chondroitin sulphate standard line (Sigma-Aldrich, C4384) with polynomic properties [60]. GAG content was corrected for the DNA content of the micro-aggregates (µg GAG per µg DNA).

Reverse transcriptase-quantitative polymerase chain reaction analysis

Two pellets per condition from the final optimisation spheroid culture experiment (21 days TGF-β (5 ng/mL) and 7 days TGF-β (5 ng/mL) followed by 14 days BMP-4 (20 ng/mL)) are washed one time in PBS and stored dry at -80 C°. Pellets are snap-frozen in liquid nitrogen and crushed using a pestle (Argos Technologies Inc, 9951901) until a powder substance is obtained. Total RNA was isolated from the pooled fraction using the RNeasy microkit (Qiagen, 74004) including an on-column DNase step, according to the instructions provided by the manufacturer. RNA was quantified using a NanoDrop ND-1000 spectrophotometer (Isogen Life Science) and cDNA was synthesized using the iScript cDNA synthesis Kit (Bio-Rad).

RT-qPCR was performed using IQ SYBRGreen supermix (Bio-Rad) and the BioRad CFX-384 cycler for chondrogenic lineage-specific primers (**Table 2**). Primers were designed using PerlPrimer v1.1.21 software and were based on sequences available in the public database of NCBI. Optimal Tm was determined using a gradient RT-qPCR and the formed product was validated via gel-electrophoresis analysis and product-specific sequencing. Relative gene expression was calculated using the efficiency corrected delta-delta Ct method by normalizing gene expression for three reference housekeeping genes and comparison to the expression on day 1 of each culture condition.

Marker	Gene	Primer sequence	Amplicon size (bp)	Annealing temperature (C)	Accession no.
Chondro-genic	Col10a1	GCAGAGGAAGCCAGGAAAG CTCTTTATGGCGTATGGGATG	111	64.2, 63, 60.3, 55.7 to 57.1	NM_009925.4
	Col2a1	CGAGGTGACAAAGGAGAATCTG CAGAAGCACCCTGATCTCCA	122	63 to 66.5, 60.3, 58, 57.1, 56.3	NM_031163.4
	Mmp13	CCTAAGCATCCCAAAACACC AACATAAGGTCACGGGATGG	218	60.3 to 65, 58, 57.1, 55.7	NM_008607.2
	Opn	CCCGGTGAAAGTGACTGATT GGCTTTCATTGGAATTGCTT	191	59.1 to 66.8	NM_001204203.1
	Sost	ACAACCAGACCATGAACCG TCAGGAAGCGGGTGTAGTG	113	65.9 to 66.4, 59.1, 60.3, 57.1	NM_024449.6
	Acan	GACACTTTCACATGCTTATGCCT CGGTAACAGTGACCCTGGA	106	60.3 to 61.8, 55.2	NM_001361500.1
	Col1a1	CTGGTTCTCCTGGTTCTCCT CGTTGAGTCCGTCTTTGCC	209	63	NM_007742.4
	Sox9	CCCGATTACAAGTACCAGCC CCCTGAGATTGCCCAGAGTG	190	65.8 and 61.6	NM_011448.4
House keeping	HPRT	GTGATTAGCGATGATGAACCA CAAGTCTTTCAGTCCTGTCCA	123	55 to 63.5	NM_013556.2
	Tbp	GCCAAGAGTGAAGAACAATCCA GCCTTATAGGGAACTTCACATCAC	138	62	NM_013684.3
	YWHAS	AACAGCTTTCGATGAAGCCAT TGGGTATCCGATGTCCACAAT	119	64	NM_001356569.1
	HMBS	CTGTTCAGCAAGAAGATGGTC TGATGCCCAGGTTCTCAG	100	57.5 to 63.5	NM_001110251.1

Table 2: RT-qPCR primers used to validate chondrogenic maturation of ATDC5 cell micro-aggregates

2.3: Results

First optimisation experiment:
In order to determine optimal culture conditions for driving chondrogenic maturation in ATDC5 cell spheroids and micro-aggregates, a large-scale culture experiment with three different media conditions (NM, AM and AM+; **Table 1**), two different culture methods (normoxic and hypoxic culture conditions), and two different spheroid sizes (35.000 and 100.000 cells). Glycosaminoglycan production and morphology were first assessed via Toluidine Blue staining (**Figure 1**). GAG production is visibly increased as a result of the extra addition of proline, dexamethasone, AsAp and TGF-β compared to the control group with no extra addition of media components (NM). The control media (NM) resulted in no GAG production within 14 days in all culture conditions. There is no visible difference in GAG production as a result of FBS addition to the differentiation medium. Spheroids (100.000 cells) and micro-aggregates (35.000 cells) cultured in hypoxic conditions remained smaller (**Figure S2**) and produced fewer GAGs compared to the equivalent spheroids and micro-aggregates cultured in normoxic conditions but do show more vacuolated cells compared with normoxic culture conditions (**Figure 1**). Lastly, the spheroids cultured under normoxic conditions show large necrotic centres on day 14, which is not observed in hypoxic conditions.

Qualification and quantification of proteoglycan content
In the second experiment, the production of GAGs in first observed on day 7 as a result of TGF-β stimulation. Micro-aggregates stimulated with BMP-4 first show GAG production on day 14 (**Figure 2A, B**). GAG production increases gradually over time in all conditions as observed in histological staining which is confirmed in the DMMB assay (**Figure 2C**) except for TGF-β (50 ng/mL). This latter condition shows a drop in GAG presence on day 21 (**Figure 2A, B**). GAG per DNA content, as measured in the DMMB assay, confirmed the results of the staining; GAG/DNA is higher in TGF-β (5 ng/mL) stimulated micro-aggregates compared with BMP-4 (50 ng/mL) stimulated micro-aggregates. DNA content increased the most as a result of high concentration BMP-4 (50 ng/mL) stimulation which is not observed in the lower concentration (20 ng/mL). This increase in DNA is comparable to the increase in size of the micro-aggregates as a result of BMP-4 stimulation (**Figure S3**). BMP-4 stimulation induces the formation of more vacuolated cells on day 21 compared to when micro-aggregates are stimulated with TGF-β. Ultimately, GAG content is higher when micro-aggregates are first stimulated with TGFβ for 7 days and compared to only adding BMP-4 while there is no obvious difference seen in vacuolated cell morphology on day 21 of culture (**Figure 2A, B**). This is however not confirmed in the GAG/DNA assay (**Figure 2C**).

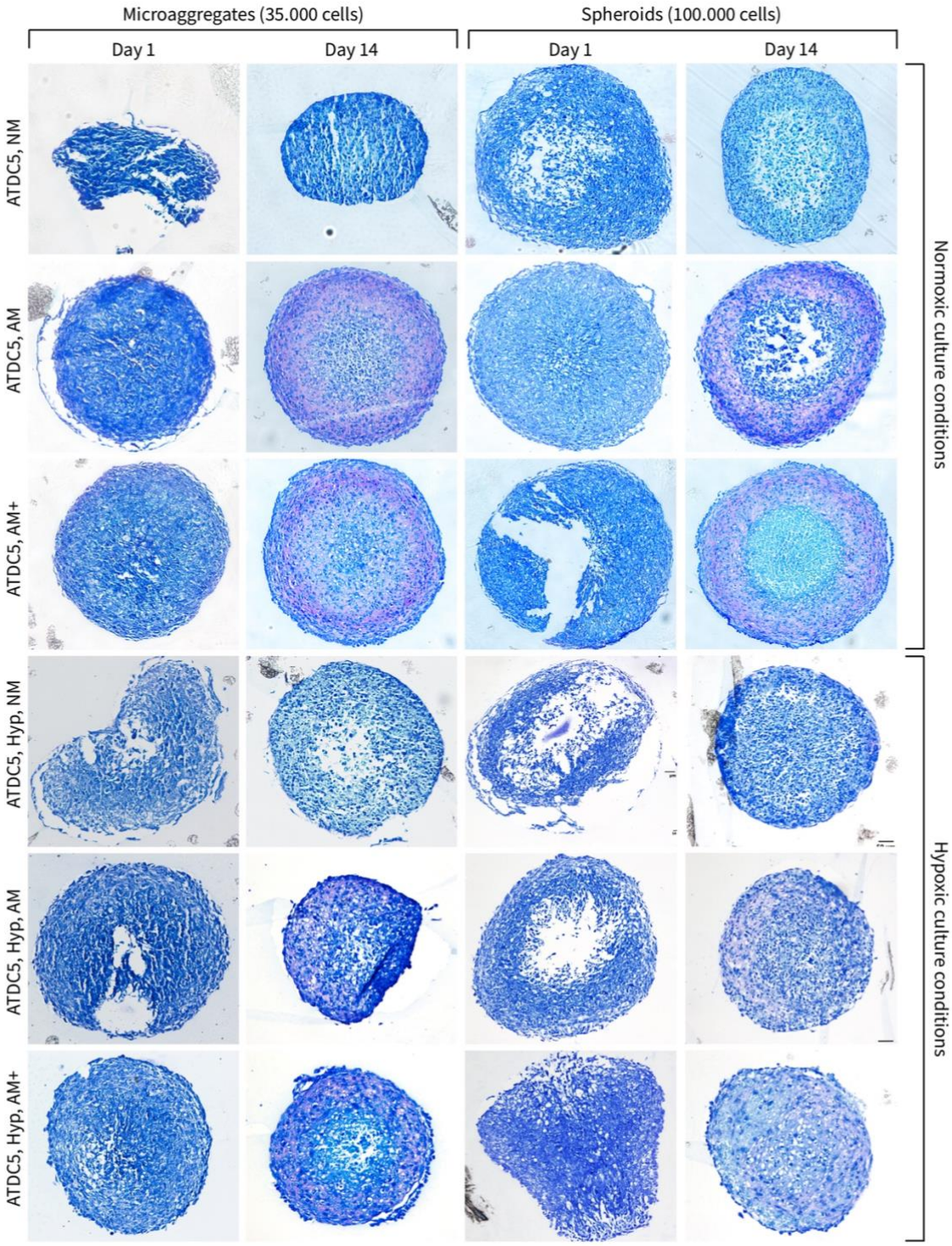

Figure 1: First optimisation experiment. Toluidine Blue staining of ATDC5 spheroids and micro-aggregates cultured under different conditions. Media compositions are mentioned on the left. Exact media compositions can be found in Table 1. Culture conditions are mentioned on the right. Normoxic culture conditions are 20% O_2 and 5% CO_2. Hypoxic culture conditions are 5% O_2 and 5% CO_2. Pellet size and culture period are mentioned at the top.

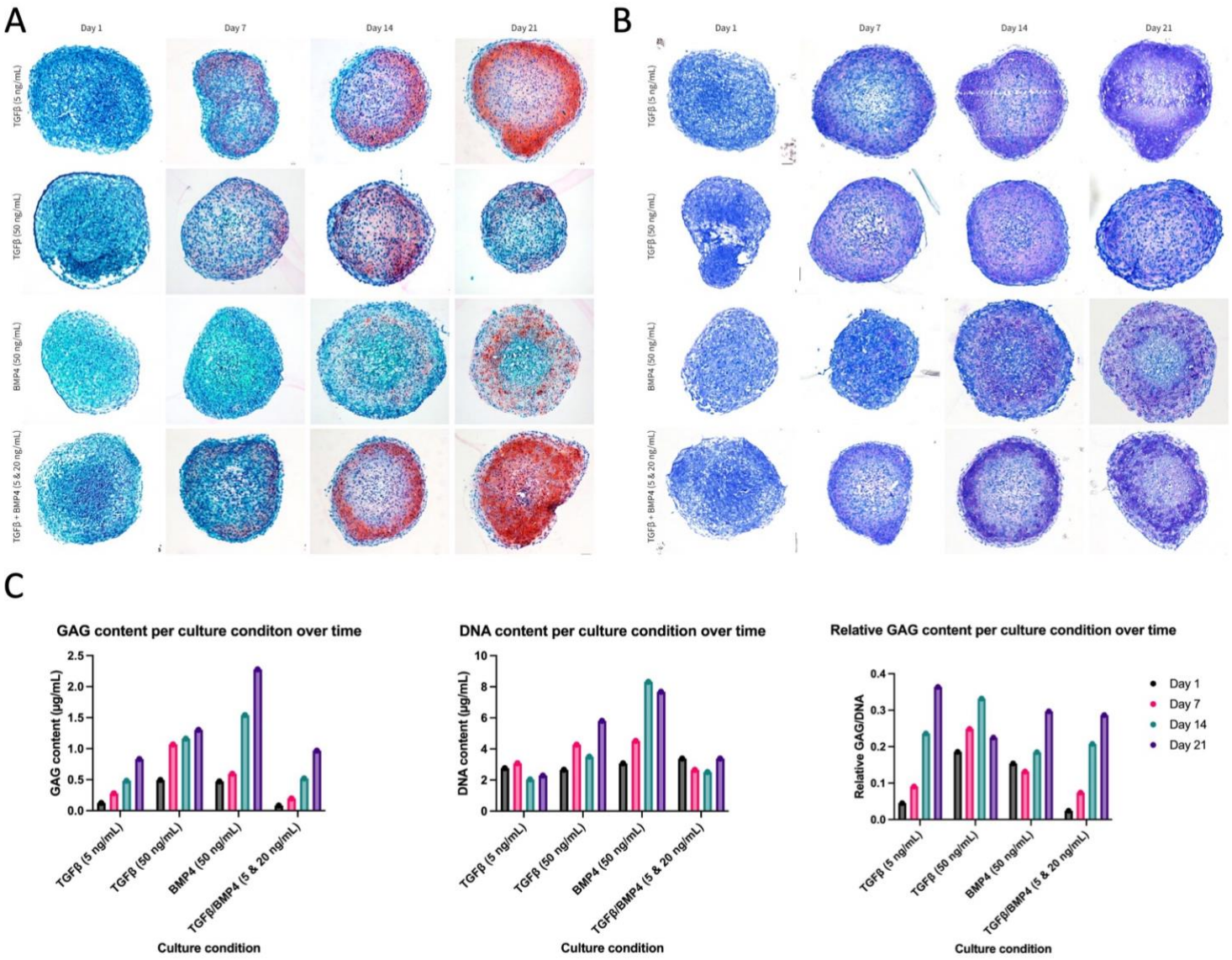

Figure 2: Analysis of GAG production by ATDC5 micro-aggregates cultured under different conditions. A) Safranin-O staining of micro-aggregates cultured for 21 days under 20% O2 in four different media compositions to assess GAG production over time. B) Toluidine blue staining of micro-aggregates cultured for 21 days under 20% O2 in four different media compositions to assess GAG production over time. C) DMMB assay to determine GAG content per condition (N=2) and DNA content per condition (N=2). X-axis shows the culture conditions, Y-axis shows GAG or DNA content in µg/mL. Relative GAG content is obtained by normalizing GAG content for DNA content. No statistical analysis could be performed.

Qualification of collagen content

Matrix composition is further studied via immunohistochemical analysis of collagen type I, type II, and type X deposition. *In vivo* expression of all collagen types of interest is shown in the growth plate of a piglet (**Figure 3A**). The production of collagen type II is observed in all culture conditions, although BMP-4-induced micro-aggregates appear to produce collagen type II in lower levels at day 7 compared with TGF-β induced micro-aggregates (**Figure 3B**). However, expression of collagen type II is similar in all conditions on day 21, although not quantified. Collagen type X is only produced as a result of BMP-4 stimulation (**Figure 3C**). On day 14 a small amount of collagen type X is produced, which is increased on day 21. TGF-β stimulation does not result in collagen type X production. Collagen type I is not produced in any of the conditions (**Figure 3D**).

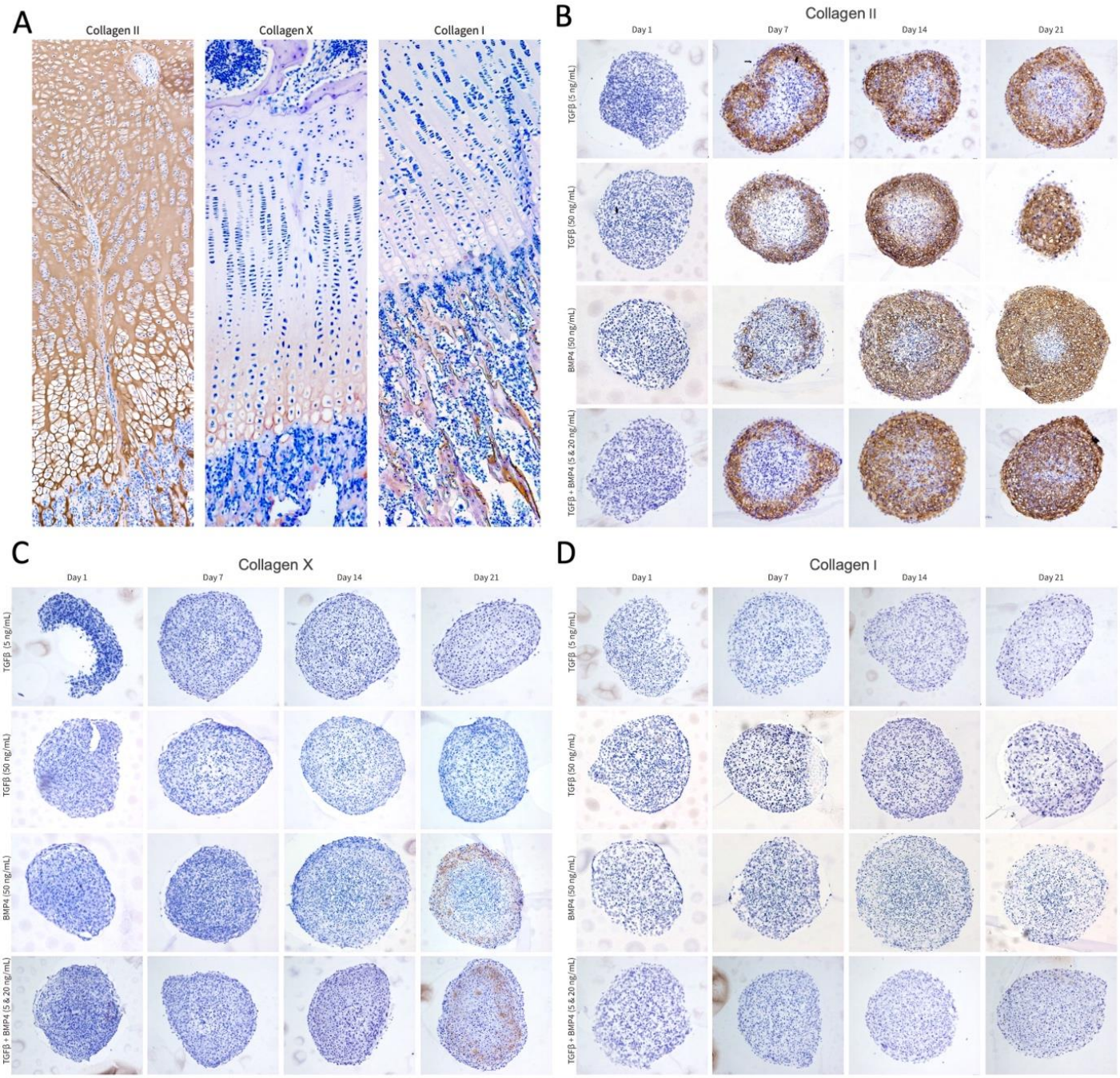

Figure 3: Collagen content of the matrix produced by ATDC5 cell micro-aggregates. A) overview of collagen I, collagen II and collagen X production in the growth plate of a piglet validated via immunohistochemical staining. This shows the localization of collagen in the matrix to show specific collagen production in different stages of chondrogenic maturation. B) collagen II production qualified via immunohistochemical staining over time. C) collagen X content of the matrix qualified by immunohistochemical staining and D) for collagen I.

Relative expression of chondrogenic genes

Relative expression of several genes involved in chondrogenic maturation and matrix production is analysed using RT-qPCR for 2 media conditions: TGF-β (5 ng/mL) and 7 days TGF-β (5 ng/mL) followed by 14 days BMP-4 (20 ng/mL) (**Figure 4**). *Col2a1* is upregulated compared to day 1 in both culture conditions on day 14 and increases further on day 21. Since the expression is compared to day 1 expression this result can be a validation of the qualitative collagen type II production. *Acan* is expressed in both culture conditions. *Sox9* and *Mmp13* expression only increases over time as a response to TGF-β + BMP4 stimulation but is not increased in expression when micro-aggregates are only stimulated with TGF-β. Collagen type X production was only observed in BMP-4 stimulated samples, which is confirmed in the relative expression of *Col10a1*. Although qualitative collagen type X production is not observed when micro-aggregates are only stimulated with TGF-β, there is an increase in *Col10a1* expression. *Col1a1* is not expressed in both culture conditions.

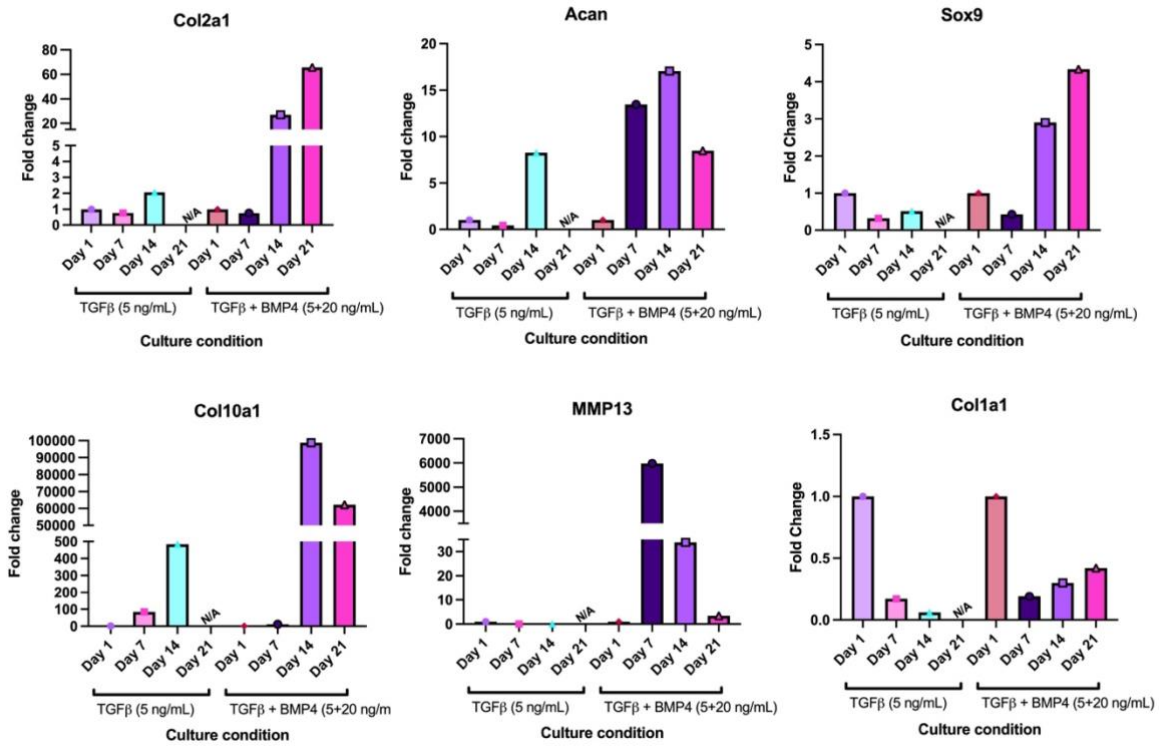

Figure 4: Relative gene expression analysis of ATDC5 micro-aggregates. Culture conditions are shown on the X-axis and consist of 21 days of TGF-β (5 ng/mL) or 7 days of TGF-β (5 ng/mL) followed by 14 days BMP-4 (20 ng/mL). ΔΔCt method is used to calculate relative expression. Three reference genes were used. Relative expression is compared with expression on day 1. Y-axis displays the fold change.

2.4: Discussion and concluding remarks

This study developed a 3D *in vitro* model of the growth plate in which chondrogenic maturation and hypertrophic differentiation are simulated over time using the ATDC5 chondrogenic cell line. This is done with the goal to replace animal models to allow for a more accessible way to study the processes behind endochondral ossification. Several optimisation steps were necessary to achieve the desired result. In the initial phase of the experiment, the desired outcome consists of matrix production rich in collagen type II and GAGs by the ATDC5 model, as well as continuous proliferation. Toluidine Blue staining revealed that GAG formation is driven by the full chondrogenic differentiation medium consisting of ITS+ premix, Dexamethasone, AsAp, proline and TGF-β regardless if FBS is added to the media or not when cultured under normoxic conditions. This was confirmed by an increase in *COL2A1* and *ACAN* expression as a result of stimulation with the full chondrogenic medium. On the contrary, medium supplemented with just ITS+ premix was not able to induce the production of GAGs. In other studies, the addition of just ITS to the culture media is sufficient in stimulating ATDC5 cells to produce GAGs in 2D culture [61,62]. The main difference in this work is that this model is a 3D model. This might influence the insulin concentration needed to reach all the cells and induce GAG production. Masuda *et al,* 2012 also reached GAG formation by solely adding 10 µg/mL insulin to ATDC5 3D micro-aggregates. The difference with this study is that the micro-aggregates consist of 1000 cells whereas the micro-aggregates in this study consist of 35.000 cells. The micro-aggregates in this study are not only larger but also received 6.25 µg/mL insulin. The difference in dose can explain why no GAGs are formed here after induction with ITS+ premix. In short, TGF-β supplemented chondrogenic medium can induce GAG production in the ATDC5 cell line in a 3D culture model.

Furthermore, a good chondrogenic differentiation was not reached in hypoxia, which was confirmed by low levels of GAG staining and a smaller pellet size. Nonetheless, hypoxic culture conditions did result in larger vacuolated cells compared to pellets cultured in normoxia. As chondrocytes in the growth plate are exposed to severe hypoxia in vivo [12,63,64], this could explain the hypertrophic morphology of the cells in the hypoxic ATDC5 cell pellets. In MSCs, it has been found that low oxygen tension resulted in better chondrogenic differentiation [63,65]. However, in ATDC5 cells, the GAG production seems to be limited in hypoxic cell culture [66]. As the production of collagen type X was not found, it seems that the vacuolated morphology could also be caused by something else (**Figure S1**). Unfortunately, it was not possible to perform quantitative PCR on these samples. Therefore, it cannot be assessed if hypoxic culture conditions did affect the upregulation of *COL10A1*. Furthermore, a longer culture period might have shown collagen X production eventually in hypoxic conditions, however, due to the lack of qPCR results, it is not possible to say. However, based on these findings it can be concluded that hypoxia has no significant stimulating effect in driving chondrogenic differentiation in the ATDC5 cell line.

Regarding the spheroid size, necrotic centres were present in the spheroids consisting of 100.000 cells. These were not present in the smaller micro-aggregates. This could be explained due to the lack of perfusion in 3D culture models. The cells rely solely on nutrient uptake via diffusion. This leads to a nutrient gradient that in larger spheroids, cannot reach the centre. This is accompanied by a build-up of waste which ultimately leads to the necrosis seen in the centre of the spheroid [43,67]. Since there was no clear difference in matrix production between the micro-aggregates and the spheroids, this finding suggests that smaller spheroid sizes handle the culture conditions better. These first experiments confirmed that culturing micro-aggregates in normoxia with full chondrogenic media gives the best result in achieving chondrogenic maturation in the ATDC5 cell line.

The second aim of this study was to investigate if the ATDC5 cell line could be driven to hypertrophic differentiation, including a morphology with larger vacuoles and collagen type X-rich matrix production. Collagen type X production was not yet reached with the initial chondrogenic differentiation medium. BMP-4 stimulation was investigated to determine its potential in driving chondrogenic maturation to the stage of hypertrophy. The addition of BMP-4 (50 ng/mL) to the differentiation medium resulted in a later-on set in GAG production compared with TGF-β stimulated micro-aggregates. In addition, stimulation with BMP-4 induced a hypertrophic phenotype as well as collagen type X production in the ADTC5 micro-aggregates. This finding is in line with the hypothesis that TGF-β stimulation drives the first stage of chondrogenic maturation including GAG and collagen type II production, whereas BMP-4 drives the later stage of chondrogenic differentiation and collagen type X production [21,22,68]. This hypothesis was confirmed with the fourth culture condition in which the micro-aggregates were first stimulated with TGF-β (5 ng/mL) for 7 days followed by 14 days of BMP-4 stimulation (20 ng/mL). First, GAG production was induced during the first 7 days, thereby reaching the first stage of chondrogenic maturation. Secondly, cells start to increase in size and have large vacuoles which is accompanied by collagen type X production during the following 14 days. This way of culturing leads to a more uniform distribution of matrix production, rather than the matrix being generated on the edges of the micro-aggregates. This could be explained by the higher metabolic activity of the cells on the edges. The more uniform distribution of matrix in the micro-aggregates stimulated with both TGF-β and BMP-4 could be a sign of better differentiation toward a chondrogenic phenotype showed as a better adjusting to the hypoxic environment. An explanation for this can be found in the growth plate. A large part of endochondral ossification occurs under hypoxic conditions in the growth plate. These maturing cells thrive under extremely low oxygen levels and adjust their metabolism to anaerobic processes for matrix production [63]. Furthermore, stimulating the micro-aggregates with BMP-4 caused an increase in *MMP13* expression. This gene encodes a metalloprotease that is responsible for breaking down the collagen type II-rich matrix to make space for collagen type X production. The expression of this enzyme is essential in reaching the hypertrophic stage in chondrogenic maturation. All these findings together showed that stimulating the ATDC5 micro-aggregates with TGF-β and BMP-4 for 21 days resulted in collagen type X production and a morphology shift to cells with larger vacuoles.

Nevertheless, collagen type X production is still limited when compared with collagen type II production. This suggests that improvement in hypertrophic differentiation can still be reached. The expression of *COL10A1* did increase on day 14, with the levels still being high on day 21. Culturing the ATDC5 micro-aggregates with BMP-4 stimulation over a longer period might show an increase in collagen type X production which is a sign of hypertrophic differentiation. Furthermore, the use of different BMPs might influence the hypertrophic differentiation of the ATDC5 cell line. Nilsson *et al,* 2007 studied the expression of different BMPs across the growth plate [69]. This study revealed that BMP-4 is not expressed as high as other BMP agonists like BMP-2 and BMP-6. Keeping this in mind, utilizing BMP-2 and/or BMP-6 might result in better hypertrophic maturation. BMPs work in the growth plate by forming a gradient of BMP agonists and antagonists (**Figure 5)**. Simulating the BMP gradient over time by starting with BMP-3, followed by BMP-7 and ending in BMP-2, 6, or 4 could be a potential method for stimulating correct hypertrophic differentiation. For this, it is important to use BMPs with a clear gradient expression. BMP-4 is an excellent candidate with the highest expression in the hypertrophic zone. On top of that, BMP-2 has very high osteogenic properties. Following BMP-4 stimulation with BMP-2 stimulation could be a driving factor in reaching trans differentiation towards osteogenesis, the last stage of endochondral ossification [18,69,70].

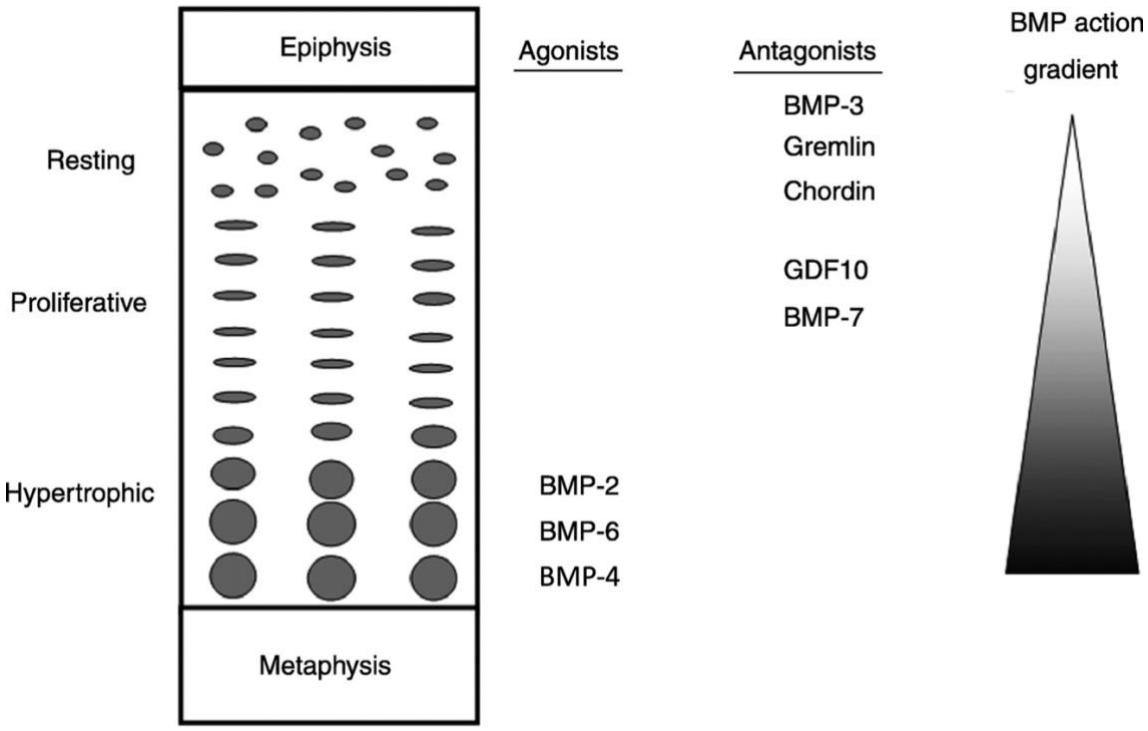

Figure 5: Overview of the bone morphogenetic protein (BMP) gradient in the growth plate. Figure adjusted from Nilsson et al, 2007 [69]

Furthermore, in this model, collagen type I was not produced by the ATDC5 micro-aggregates. There are several explanations for this result. Important to note is that collagen type I is not produced by growth plate chondrocytes but by osteoblasts in the bone. This means that to achieve collagen type I production by the ATDC5 cells, the cartilage needs to be remodelled into bone. During *in vivo* endochondral ossification, the cartilage is remodelled into bone as a result of an influx of osteoblasts and osteoclasts from the primary ossification centre. The influx is made possible by the presence of blood vessels allowing perfusion of the tissue. In the *in vitro* model developed in this study, there is no perfusion possible which means that osteoblasts cannot remodel the cartilage into bone [11]. However, Lamandé *et al*, 2023 has shown that chondrocytes are capable of trans differentiation to osteoblasts, facilitating bone remodelling *in vitro* [71]. This study is conducted with induced pluripotent stem cells (iPSCs) over a culture period of 73 days. Although this is not yet proven in the ATDC5 cell line, it does prove that hypertrophic chondrocytes can transition into osteoblasts *in vitro* which is an interesting outcome to achieve in a 3D *in vitro* model of the growth plate.

Nonetheless, this study has its own set of limitations. 3D *in vitro* culture models using a immortalized cell line like the ATDC5 cell line, are unable to show the later stages of chondrogenesis that *in vivo* results in bone elongation [34,35]. Another limitation of 3D culture is that the culture model is not perfused [43]. This causes a nutrient gradient which does not allow similar treatment of all cells in the micro-aggregate. This often results in necrotic centres surrounded by fast-proliferating cells on the edge of the aggregate. This results in a skewed matrix deposition accompanied by a lack of cellular organization compared to the *in vivo* situation [13,36]. Moreover, this study is conducted with the ATDC5 cell line. This cell line is an immortalized cell line which is an immortalized cell line originating from the mouse species [45]. Immortalized cell lines are modified to divide infinitely which is achieved via genetic changes [72]. This could mean that these cells respond differently to stimuli compared to the situation *in vivo*. Furthermore, the goal of this study is to model endochondral ossification for the purpose of developing new regenerative strategies in cartilage and bone regeneration in humans. The mouse species is not the most representative species to study the growth plate since the growth

plate does not close upon maturation in contrast to the human growth plate [40,73]. This means that the regulation of the growth plate between mice and human differs greatly. Future work could focus on using a cell type more representative of the human growth plate in an approach to model endochondral ossification *in vitro*.

Altogether, this study has shown that the ATDC5 cell line can be driven to chondrogenic maturation over time via TGF-β and sequential BMP-4 stimulation in a 3D culture system. These findings suggest that in general, the ATDC5 cell line can be induced to simulate the first stages of endochondral bone formation *in vitro* including the hypertrophic phase but excluding trans differentiation. This suggests that the present study lays the groundwork for future *in vitro* modelling of the growth plate using different cell types to achieve a closer resemblance to the growth plate *in vivo*.

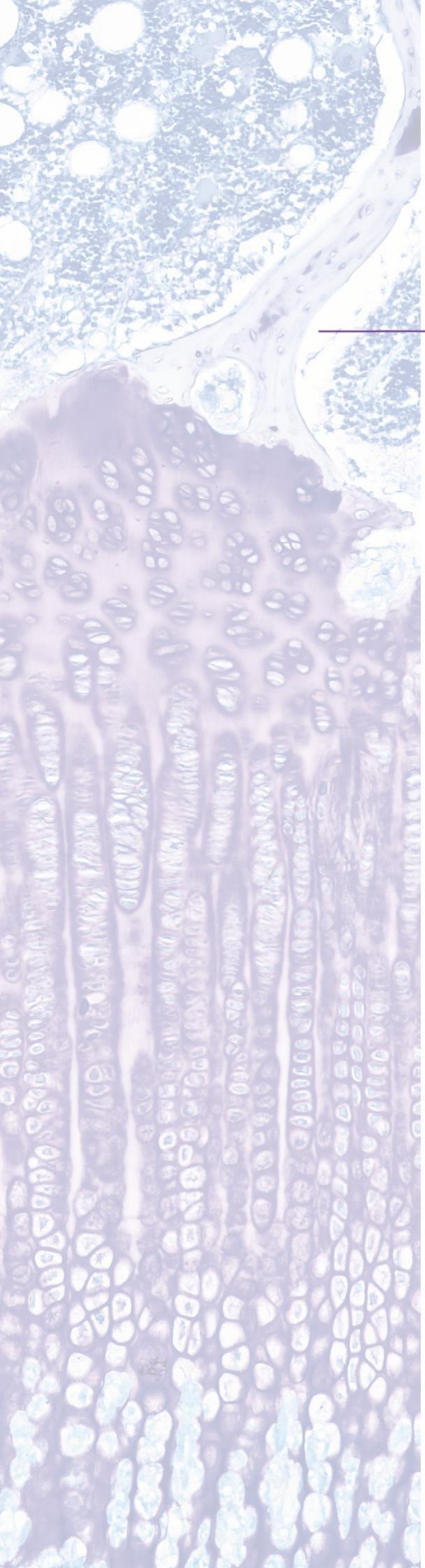

Chapter 3

Unraveling Growth Plate Dynamics: Primary Cell Isolation, Resting Zone Progenitor Marker Unveiling, And Spatial Gene Expression Analysis

3.1: Introduction

Musculoskeletal diseases like trauma, (lower) back pain, and arthritis are the number two cause of years lived with disability worldwide [74,75]. As the prevalence and severity of these diseases increase with age, this burden on society will only increase with the increased ageing in the Western world. One of the causes behind musculoskeletal disease is tissue degeneration of cartilage which results in loss of function of the tissue which is often paired with a lot of pain. Current treatment options can help with pain management and prevent further degeneration of the tissue [1,6,76–79]. However, these treatments are often not curative. All of these diseases highlight the critical need to develop novel regenerative strategies targeting cartilage and bone.

As mentioned before in **Chapter 1**, current strategies for regenerating bone often fail due to the hypoxic environment of the tissue. Endochondral ossification, a process in which bone is formed using a chondrogenic template, occurs largely under hypoxia. This renders this method of ossification an interesting subject to study for new approaches in the development of regenerative strategies. A tissue in which endochondral ossification occurs during post-natal development is the growth plate. This tissue poses the perfect template to study the formation and maturation of cartilage and eventually the remodelling into bone. The growth plate can be divided into three different zones, the resting, proliferative, and hypertrophic zone, each containing chondrocytes in different stages of maturation (**Figure 1**). The resting zone contains relatively inactive progenitor cells that replenish the growth plate. The proliferative zone contains fast replicating chondrocytes appearing in longitudinal columns that secrete matrix rich in collagen type II and GAGs. The hypertrophic zone contains large vacuolated cells that secrete matrix rich in collagen type X before undergoing apoptosis or transdifferentiating into osteoblasts to facilitate the remodelling of the cartilage template into bone [12,80].

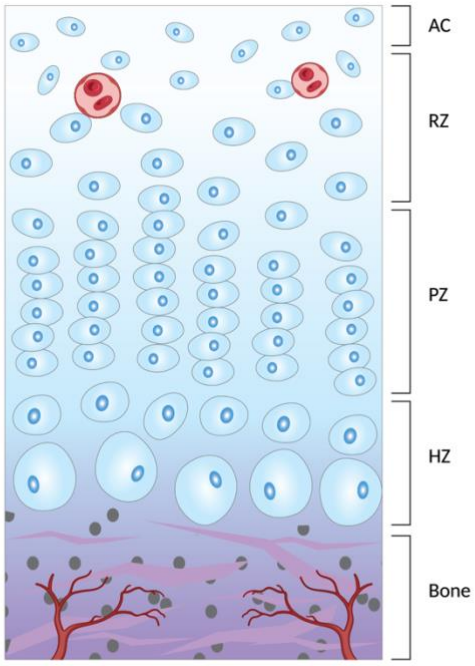

Figure 1: Schematic overview of the composition of the epiphyseal growth plate. AC = articular cartilage, RZ= resting zone, PZ = proliferative zone, HZ = hypertrophic zone. Figure created with BioRender and Adobe Illustrator

An exciting tool in unravelling the mysteries behind endochondral ossification in the growth plate is the study of adult height variation. Variation in adult height is a highly genetic trait resulting in differences between individuals [81,82]. Studying these differences and how these translate to extended chondrocyte proliferation and ossification can create an excellent opportunity to identify new targets for regeneration targeting cartilage and bone. Dogs and pigs show extreme intra-species height variation between small and large breeds. Compare for example a Pomeranian with a Great Dane with an average Whiters height of 23 and 81 cm respectively [83]. This renders the canine and porcine growth plate specifically an excellent tool for studying differences in adult height. Determining differences in growth plate regulation between large and small breeds could help in identifying important genes and pathways in growth plate regulation. Understanding the involvement of these genes in endochondral ossification could be a game-changer in stimulating the regeneration of cartilage. Furthermore, dogs and pigs can be used as a more translatable model for studying the human growth plate compared to rodents, which are currently mainly used to study endochondral bone formation [73,84,85].

Using the dog and pig species as a model to study endochondral ossification occurring in the growth plate requires the sacrifice of these animals. Concerning the 3Rs principle, animal sacrifice should be kept to a minimum [33]. As mentioned before in **Chapter 2**, three-dimensional *in vitro* modelling can be utilized to replace animal models and allows for studying the dynamics and mechanisms in the growth plate in a more accessible manner. However, utilizing the correct cell type is critical in developing an accurate model. Dog primary growth plate cells, or even solely the resting zone progenitor cells are excellent candidates for the 3D culture model. The first challenge in this is identifying and isolating the progenitor cells that reside in the resting zone. As of now, the stem cells of the growth plate have not been identified or isolated yet in larger animals like pigs and dogs. Nonetheless, several markers have been described that could help in identifying these cells, of which CD146 and CD105 are the most promising [86–90]. Furthermore, specificity for the resting zone progenitor cells can likely be increased by using mesenchymal stem cell markers like CD73, CD44, CD90, and CD271 [91,92].

This project aims to develop an *in vitro* cell culture model in which the progenitor cells of the growth plate itself are used to recreate an *in vitro* growth plate. To obtain this goal, two research objectives were formulated: 1) how can we identify the progenitor cells of the growth plate, and 2) what is the optimal 3D culture protocol for primary growth plate cells. The first objective will be investigated using immunohistochemical analysis and RT-qPCR for the markers CD146, CD105, CD73, CD271, CD44 and CD90. For the second objective, canine and porcine, the latter with better availability, will be cultured in different culture conditions. I hypothesize that TGF-β and BMP-4 stimulation can be used to achieve chondrogenic maturation and hypertrophic differentiation as seen in the ATDC5 cell line. Hypertrophic differentiation would be validated with collagen type X production.

3.2: Material and methods

Primary tissue collection
Growth plates were collected from the ribs of piglets between 5 and 10 weeks old euthanized for various diseases and pups of around 12 weeks of age at the pathology department of veterinary medicine, Utrecht University as quickly as possible after euthanasia. The growth plates were harvested from the ribs using a table saw to create manageable pieces of around 50 mm thickness and collected in DMEM-F12 (Gibco, 11540446) supplemented with 1% penicillin/streptomycin (P/S; GE Healthcare Life Sciences) before further digestion and isolation of primary growth plate cells. Other growth plates were harvested and fixed in formalin followed by EDTA decalcification for histological analysis.

Isolation of growth plate cells from primary tissue
Further processing of the tissue consisted of precision excision of the growth plate section using an inverted stereomicroscope (Breukhoven microscope systems, Iso9001) and a sterile scalpel blade nr.15 (Swann Morton, 0205). The growth plate sections were further digested either by 30-minute incubation at 37 C° with 3,75 mg/mL pronase (Roche Diagnostics, 11459643001) in DMEM-F12 (Gibco, 11540446) followed by overnight incubation with 2,5 mg/mL collagenase II (Worthington, 43D14200A) in DMEM-F12 (Gibco, 11540446) at 37 C° [60] or by 30-minute incubation with collagenase IV (Sigma-Aldrich, 9001121) at 37 C° followed by overnight incubation at 37 C° with collagenase II (Worthington, 43D14200A) to optimize the digestion method [93].

3D culture of primary canine growth plate cells
Primary growth plate cells were cultured in T25 flasks to ensure cell-cell contact to improve proliferation. Cells are passed once (P1) before usage in a 3D culture experiment to ensure cell viability and proliferation capacity. Primary growth plate cells from canine origin were released from T25 flasks using TripLE™ Express Enzyme (1X, Gibco, 12604013), centrifuged at 500*g* for 5 minutes and resuspended in DMEM-F12 medium containing 1% P/S. Micro-aggregates were firmed by seeding 35.000 cells per well in an ultra-low attachment U-bottom 96 well plate (Costar, 28022057) in 100 µL chondrogenic differentiation medium consisting DMEM/F12 supplemented with proline (40µg/mL, Sigma-Aldrich, 147853), ascorbic acid 2-phosphate (0.2 mM, Sigma-Aldrich, 1713265258), dexamethasone (200 nM, Sigma-Aldrich, 50022), and TGF-β (5 or 50 ng/mL, R&D Systems, 240-B) or BMP-4 (20 or 50 ng/mL, Gibco, PHC9533). The micro-aggregates self-assembled within 24 hours. The medium was refreshed every 2-3 days and micro-aggregates were collected on day 1, day 7, day 14, and day 21 for histological analysis (N=2) and GAG/DNA analysis (N=2).

Histological staining to qualify GAG content in the matrix
Two spheroids per condition were fixed overnight in 4% paraformaldehyde with 1% Eosin (Merck, 115935) dissolved in PBS directly after retrieval at each time point. After fixation the spheroids were incorporated in 3% agarose and dehydrated using a sequential ethanol series in a tissue processor after three days of fixation maximum, ending in paraffin in which the samples are embedded. 5 µm sections were cut using a microtome. Before staining, sections were rehydrated using xylene followed by a graded ethanol series (100%, 96%, 70%). Glycosaminoglycans were visualized with a toluidine blue, and safranin O/Fast green staining was performed according to the protocol provided in **Chapter 2**.

Immunohistochemical staining to qualify the collagen content of the matrix
Immunohistochemical evaluation for collagen type I, type II, and type X was performed according to the protocol provided in **Chapter 2**.

DNA and GAG content analysis

Two pellets per condition were pooled together and digested overnight in papain digestion solution consisting of 10 mM Papain (Sigma-Aldrich, P3125), 10 mM Cysteine HCL (Sigma-Aldrich, C9768-5G), 200 mM H_2NaPO_4*2 H_2O (Boom, 21254), and 10 mM EDTA (Merck Millipore, 100944) at 60 C°. The DNA content of the microaggregates was measured using the Qubit dsDNA High Sensitivity Kit (Invitrogen, Q32851) according to the instructions from the manufacturer. To quantify the GAG content in the microaggregates, a dimethyl methylene blue (DMMB) assay was performed with the papain digested samples. After the addition of DMMB solution, the absorbance was immediately measured (540/595 nm) using a microplate multimode plate reader (VANTAstar, BMG Labtech). The GAG content was validated based on a chondroitin sulphate standard line (Sigma-Aldrich, C4384) with polynomic properties [60]. GAG content was corrected for the DNA content of the microaggregates (µg GAG per µg DNA).

Immunohistochemical staining of surface markers

Growth plate tissue was fixed in 4% paraformaldehyde for 7 days followed by decalcification in 0,5M EDTA. Decalcification is continued until the growth plate tissue is easily pierceable with a needle. After decalcification, the tissue was dehydrated in sequential ethanol series in a tissue processor ending in paraffin in which the tissue was embedded. 5 µm sections were cut with a microtome (Leica).

Immunohistochemical staining was performed for surface markers of interest (**Table 3**). Sections were deparaffinized using xylene (Klinipath, 4055-9005) and a gradual ethanol series (100%, 96%, 70%) and were washed with 0,1% PBS-Tween twice for 5 minutes (Boom, 76021765) followed by a 0,3% H_2O_2-PBS block of 10 minutes. Sections were blocked with 5% BSA in PBS for 15 minutes at room temperature. Thereafter, sections were incubated with a target primary antibody (**Table 3**) overnight at 4 °C. Sections were incubated with the corresponding secondary antibody conjugated with HRP for 30 minutes at room temperature (**Table 3**). After washing with PBS, the sections were incubated with Bright DAB Substrate Kit (Immunologic, BS04-110) for a maximum of 5 minutes or until brown staining appeared. The sections were counterstained with filtered Mayers haematoxylin solution (Sigma Aldrich, MHS32-1L) for 30 seconds and washed under running tap water for 10 minutes before dehydration with a graded ethanol series (70%, 96%, 100%) finishing in 2 times 5 minutes xylene. The slides were mounted with permanent mounting medium (Sigma-Aldrich, 102506567) and analysed using light microscopy (Olympus BX51).

Target	Host species	Clonality	Concentration	Brand and reference	Secondary antibody	Isotype
CD44	Rat	Monoclonal	0,5 µg/mL	Thermo Fischer Scientific, MA1-10225	Goat anti-rat IgG HRP	Rat IgG
CD73	Rabbit	Polyclonal	0,5 µg/mL	LSBio, LS-B8284	BrightVision poly HRP-Anti-Rabbit	Rabbit IgG
CD90	Rabbit	Monoclonal	1:750 dilution	Abcam, ab92574	BrightVision poly HRP-Anti-Rabbit	Rabbit IgG
CD271	Mouse	Monoclonal	1 µg/mL	Thermo Fischer Scientific, 14-9400-82	BrightVision poly HRP-Anti-mouse	Mouse IgG

Table 3: Overview of antibodies used for immunohistochemical analysis of surface marker of interest expression in the growth plate

Cryosectioning

Growth plates obtained from the ribs of piglets and pups of various genders and ages were collected in liquid nitrogen to preserve RNA integrity and embedded in Tissue-Tek O.C.T compound (Sakura, 4583) in preparation for cryosectioning before freezing and storing tissue samples at -80 °C. 50 µm cryosections were obtained using a cryotome to allow for zone-specific separation of the growth plate. However, cryosectioning of frozen tissue containing bone proved rather difficult since the bone was not decalcified before to maintain RNA integrity which caused the sections to splinter. A further optimisation step involved collecting primary growth plate tissue in RNAlater solution supplemented with 10% EDTA (dissolved at 60 °C under constant stirring for 30 minutes) with the pH set at 5.2 and allowing the tissue to decalcify at 4 °C for four days. The tissue was embedded in Tissue-Tek O.C.T compound and frozen at -80 °C until further use. Cryosections of 50 µm were successfully obtained on warmed X-tra adhesive slides (Leica Surgipath) before refreezing tissue on dry ice immediately. Cryosections were stored at -80 °C until further use.

Growth plate zone-specific RNA isolation

Porcine tissue sections obtained via cryosectioning were thawed for 60 seconds, fixed in 70% ethanol and 100% methanol. This was followed by short rehydration in 96% ethanol before staining soft tissue briefly with 0,2% Eosin (Merck, 1159350100) in 75% ethanol containing 0,5% acetic acid. Sections were washed with 70% ethanol and submerged in 100% ethanol while cutting to prevent the tissue from drying out. Staining with Eosin was performed to better visualize histological hallmarks that define the different zone in the growth plate. An inverted stereomicroscope (Breukhoven microscope systems, Iso9001) was used to visualize the different zones and dissection was performed using a small hypodermic needle and a sterile scalpel blade nr.15 (Swann Morton, 0205). Five fractions per section were isolated: bone, hypertrophic zone (HZ), proliferative zone (PZ), resting zone (RZ) and the articular cartilage (AC). Since the morphology of the canine growth plate was much better visible compared to the porcine growth plate, the canine tissue was not fixed but submerged in RNAlater to prevent drying out of the tissue during dissection. This was done with the goal to maintain better RNA integrity. Isolated growth plate sections were pooled in epps and immediately frozen. Total RNA was isolated from the pooled fraction using the RNeasy Minikit (Qiagen, 74104) including an on-column DNase step, according to the instructions provided by the manufacturer. RNA was quantified using a NanoDrop ND-1000 spectrophotometer (Isogen Life Science) and cDNA was synthesized using the iScript cDNA synthesis Kit (Bio-Rad). Primers specific for canine tissue were used after cross-referencing sequences with porcine DNA using the NCBI databank.

Quantitative PCR was performed using IQ SYBR green supermix (Bio-Rad) and the BioRad CFX-384 cycler according to the manufacturer's protocols for chondrogenic growth plate-specific genes as well as for surface markers of interest (**Table 4**). The standard line consists of a 4-fold dilution series obtained from a pool of all cDNA samples. A whole growth plate sample was simulated by pooling the different zones into one sample per species. Relative gene expression was calculated using the efficiency corrected $\Delta\Delta$Ct method by normalizing gene expression for four reference housekeeping genes (Table 4) and comparison to expression in the whole growth plate sample (GP).

Marker	Gene	Primer sequence	Amplicon size (bp)	Annealing temperature (C)	Accession no.
Growth plate specific	Col2a1	GCAGCAAGAGCAAGGAC TTCTGAGAGCCCTCGGT	150	60.5-65	NM_001006951
	Col10a1	CCAACACCAAGACACAG CAGGAATACCTTGCTCTC	80	61	XM_038684439.1
	Col1a1	GTGTGTACAGAACGGCCTCA TCGCAAATCACGTCATCG	109	61	NM_001003090
	Sox9	CGCTCGCAGTACGACTACAC GGGGTTCATGTAGGTGAAGG	105	62 + 63	NM_001002978.1
	PtHrp	GTGTTCCTGCTGAGCTACTCG ATGGGTGGTCGCCTTCTA	451	66,5	XM_038438653.1
	IHH	TCACCACTCAGAGGAGTCG GTGCTCAGACTTGACGGAG	172	60	XM_545653
	SFRP5	ACTGCCACAAGTTCCC GATCTTGGTCACTGGAGG	88	63.5	XM_543955.2
Surface markers	CD44	CTTCTGCAGATCCGAACACA GAGTAGAAGCCGTTGGATGG	147	60	XM_038423375
	CD73	CTCCAACACATTCCTTTACAC ACTCAACCTTCAAATAGCCT	150	61	XM_038675165.1
	CD90	CAGCATGACCCGGGAGAAAAAG TGGTGGTGAAGCCGGATAAGTAGA	134	63,5	NM_001287129.1
	CD271	GCCTACATTGCCTTCAAGAG AGAGATGCCACTGTCACTG	122	57-63	XM_038675121.1
	CD105	CATCCTTCACCACCAAGAG CAGATTGCAGAAGGACGG	139	60	XM_038678496.1
	CD146	GGGAATGCTGAAGGAAGG CTTGGTGCTGAGGTTCTG	99	63	XM_038664662.1
House keeping	HPRT	AGCTTGCTGGTGAAAAGGAC TTATAGTCAAGGGCATATCC	104	56+58	NM_001003357
	HMBS	TCACCATCGGAGCCATCT GTTCCCACCACGCTCTTCT	112	61	XM_038664685.1
	GAPDH	TGTCCCCACCCCAATGTATC CTCCGATGCCTGCTTCACTACCTT	100	58	NM_001003142
	YWHAZ	CGAAGTTGCTGCTGGTGA TTGCATTTCCTTTTTGCTGA	94	58	XM_843951

Table 4: List of primers containing growth plate specific genes, surface markers and house keeping genes used for RT-qPCR analysis.

3.3: Results

Qualification and quantification of proteoglycan content in the matrix

GAG content is qualified with a Safranin-O/Fast green staining and a Toluidine Blue staining (**Figure 1A, B**). Results show higher GAG production in TGF-β stimulation compared with BMP-4 stimulation. In the first case, the matrix is produced throughout the entire micro-aggregate while in case of BMP-4 stimulation, the GAG-rich matrix appears to be more centred. Quantification of GAG content in the produced matrix shows a similar pattern (**Figure 1C**). GAG content increases over time as a result of TGF-β stimulation. However, when the cells are stimulated with BMP-4, the GAG content stagnates after day 7 and remains at similar levels, lower than TGF-β stimulated micro-aggregates.

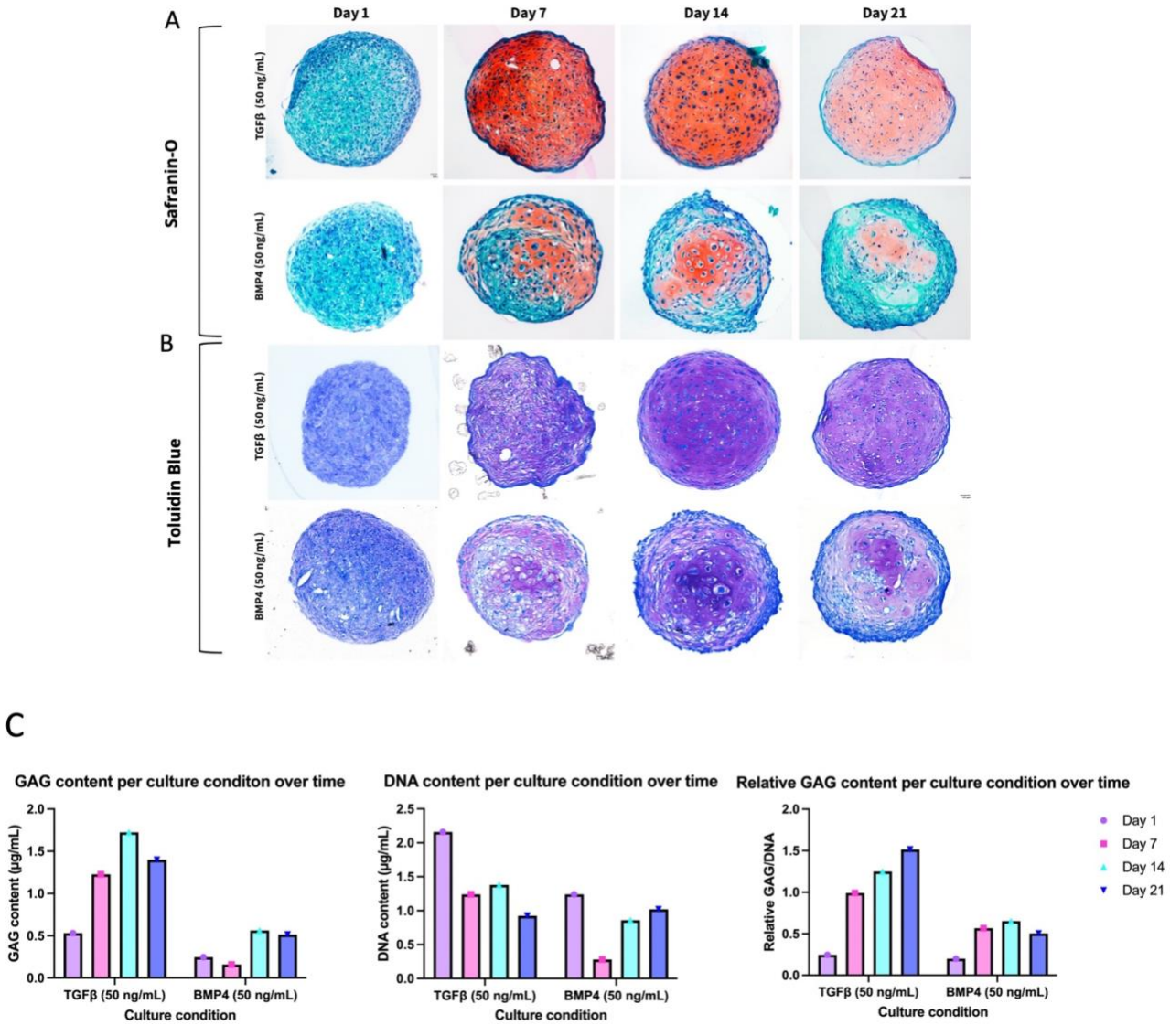

Figure 1: qualification and quantification of GAG production by micro-aggregates consisting of primary dog GPCs. A) Safranin-O/Fast green staining. GAGs are stained red. X-axis shows the time points of pellet retrieval. Y-axis shows the culture conditions. B) Toluidin Blue staining: GAGs are stained deep violet. C) GAG content, DNA content and relative GAG content per DNA produced by micro-aggregates. Relative GAG content is corrected for DNA content. X-axis displays the culture conditions. Y-axis displays GAG or DNA content in µg/mL or relative GAG per DNA. Legenda mentions time points of pellet retrieval.

Qualification of collagen content in the produced matrix

Further assessment of the composition of the matrix produced by dog GPC micro-aggregates is performed via analysis of the collagen content. Immunohistochemical analysis is performed for collagen II, X, and I (**Figure 2**). Low amounts of collagen II are already present on day 1 but increase visibly a lot during the following 7 days (**Figure 2A**). Collagen II displays a similar localisation of production compared to the GAGs, where TGF-β stimulation results in more collagen II (**Figure 1A, B**). A similar pattern is noticed in collagen I production (**Figure 2C**). Collagen I is already present in the matrix on day 1 but increases in production over time. The localisation of the collagen I-rich matrix is more on the edge of the micro-aggregates compared to the centred localisation of collagen II. There is no collagen X-rich matrix produced by the micro-aggregates (**Figure 2B**).

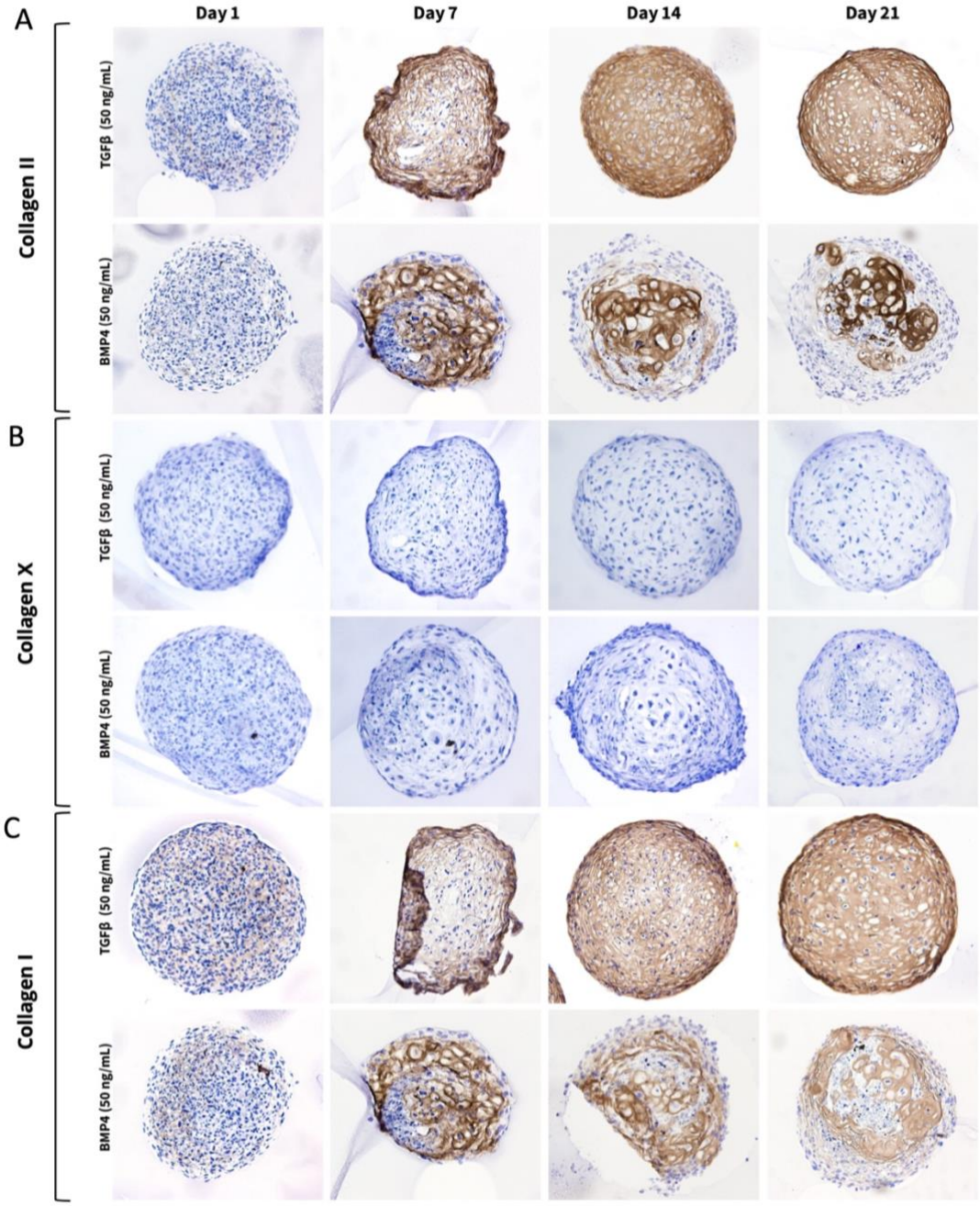

Figure 2: Qualification of collagen rich matrix production in micro-aggregates of primary dog GPCs. Culture conditions are shown on the Y-axis. Time points of pellet fixation are shown on the X-axis. A) immunohistochemical staining of collagen II. B) immunohistochemical staining of collagen X. C) immunohistochemical staining of collagen I.

Zone-specific gene expression validation

The porcine tissue was fixed and counterstained with eosin, while the canine tissue could be dissected in RNAlater solution where no fixation was necessary. RNA integrity varied between species and zones in which the RIN values for canine tissue are higher (7.70-8.70) compared to pig tissue (3.80-7.70, with two values N/A) (**Figure S4**). To validate correct separation of the growth plate zones, gene expression profiles of chondrogenic markers involved in specific stages of chondrogenic maturation are obtained (**Figure 3**). The expression of Col10a1 is an excellent marker to determine correct separation of the hypertrophic zone. In the porcine growth plate, col10a1 is indeed expressed the highest in the hypertrophic zone (HZ) with a fold change increase of 2 compared with the proliferative zone (PZ). In the canine growth plate, col10a1 is expressed throughout the whole growth plate rather than specifically in the HZ with no large differences in fold change between the RZ, PZ, and HZ. Col2a1, a marker specifically expressed by the chondrocytes in the articular cartilage (AC) and the resting zone (RZ), is expressed 30-fold higher in the AC compared to the PZ and HZ in the porcine growth plate and 7-fold in the canine growth plate. Col1a1, a marker expressed in bone, is not expressed in the porcine growth plate and is 0.5-fold higher expressed in the bone fraction. However, in the canine growth plate, col1a1 is expressed in the AC fraction with a 5-fold increase compared to the bone fraction. Sox9, a marker expressed by resting zone chondrocytes, shows a 3-fold increase in the resting zone of the porcine growth plate compared to the PZ and no concrete result in the canine growth plate. Secreted frizzled-related protein 5 (SFRP5), an RZ marker, is expressed 30-fold and 2-fold higher in the porcine and canine RZ compared to the PZ respectively. PtHrp forms a gradient with IHH. PtHrp is expressed by chondrocytes in the AC. PtHrp is expressed 80-fold higher in the AC of the porcine growth plate compared to the PZ, in comparison with the canine growth plate in which PtHrp is not expressed in the AC. IHH is then expressed by PZ and HZ chondrocytes. IHH shows a 3-fold and a 2-fold increase in expression in the PZ and HZ respectively compared to the other fractions in the porcine growth plate. In the canine growth plate, PtHrp is 5-fold and 3-fold higher expressed in the PZ and HZ respectively compared with the RZ.

Localisation of CD-marker presence in the porcine and canine growth plate

The presence of mesenchymal (CD73, CD271, CD90, and CD44) surface markers in the canine and porcine growth plate, especially the presence in the resting zone, is assessed using immunohistochemical analysis. CD73 and CD44 show no positive staining in the resting zone of both species (**Figure 4, 5**). The positive CD73 staining seen in the proliferative zone of the canine growth plate looks like aspecific background staining since the colouring is not specific on cells. CD44 in the growth plate does show specific staining of cells in and surrounding the blood vessel in the resting zone, which is not observed in the porcine resting zone. Furthermore, CD44 displays positive staining of cells in the bone marrow in both species. CD90 stains positive in cells of the resting zone and in cells in and surrounding the blood vessel. Lastly, CD271 shows positive staining in and around a blood vessel in the canine resting zone, as well as in the hypertrophic zone, whereas no positively stained cells were noticed in the porcine growth plate.

The validation of the presence and localisation of these markers in the growth plate, supplemented with CD146 and CD105, is further validated using zone-specific gene expression analysis (**Figure 6**). CD73, a mesenchymal stem cell marker, is expressed in the resting zone with a 10-fold and 11-fold increase compared to the whole growth plate in the porcine and canine growth plate respectively. CD271, also an MSC marker, is not expressed in the porcine growth plate resting zone but does show a 2.5-fold higher expression in the canine growth plate. Furthermore, CD90 has a 2.5-fold higher expression in the porcine RZ and 12-fold in the canine RZ compared to the entire growth plate. CD44, a hematopoietic lineage marker as well, is 10-fold higher expressed in the porcine and canine resting zone compared to the entire growth plate. Next, CD146, a marker that is likely present on resting zone progenitor cells is expressed 50-fold and 13-fold higher in the RZ of the porcine and canine growth plate respectively. CD105, a marker that also has the potential to mark resting zone

progenitor cells, is also expressed in the RZ of the growth plate, respectively, 10-fold and 2-fold increased in porcine and canine growth plate tissue.

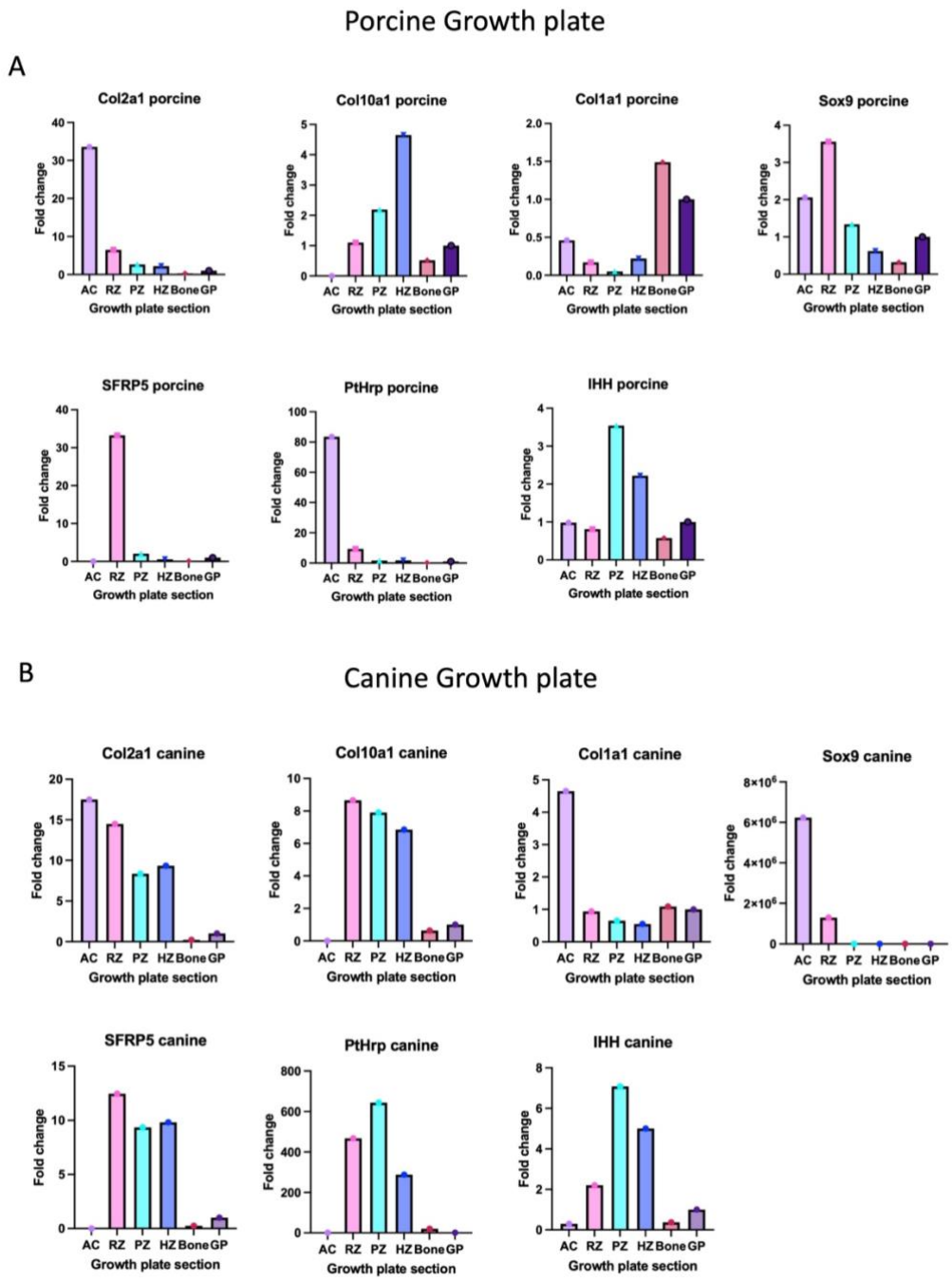

Figure 3: Relative gene expression of spatially expressed chondrogenic genes in the specific zones of the growth plate. RT-qPCR results for Col2a1, Col10a1, Col1a1, Sox9, SFRP5, PtHrp, and IHH. $\Delta\Delta$Ct method is used by comparing gene expression with 4 reference genes and to a pooled sample containing all zone fractions. A) relative expression of chondrogenic genes in the porcine growth plate and B) in the canine growth plate. Y-axis displays the Fold change and the X-axis the different growth plate zones.

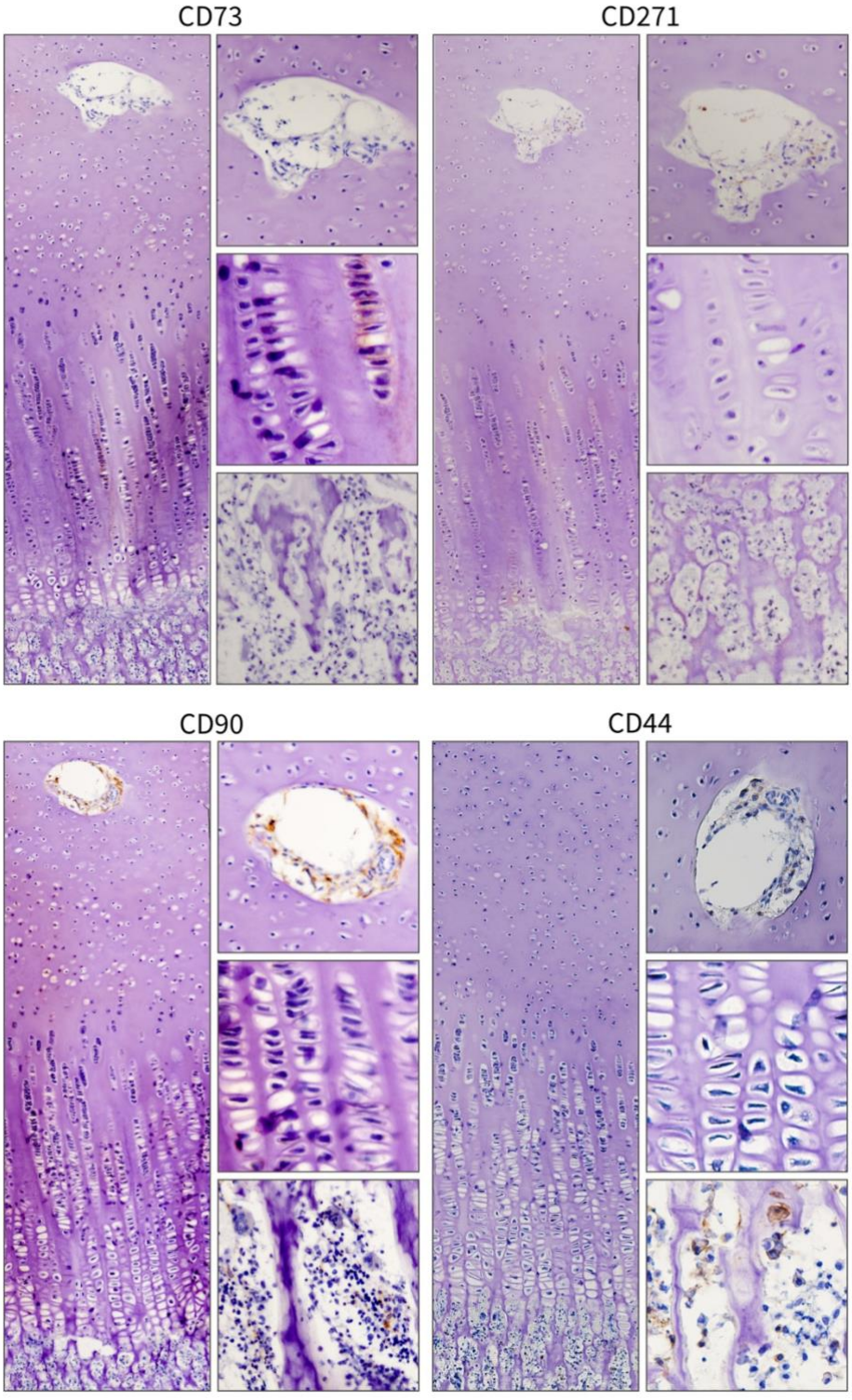

Figure 4: Qualification of CD-marker expression in the canine growth plate. The left pictures provide an overview if expression throughout the growth plate. The right images provide a zoomed in view of the resting zone, hypertrophic zone, and of the bone fraction. Immunohistochemical staining for CD73, CD271, CD90, and CD44 is shown.

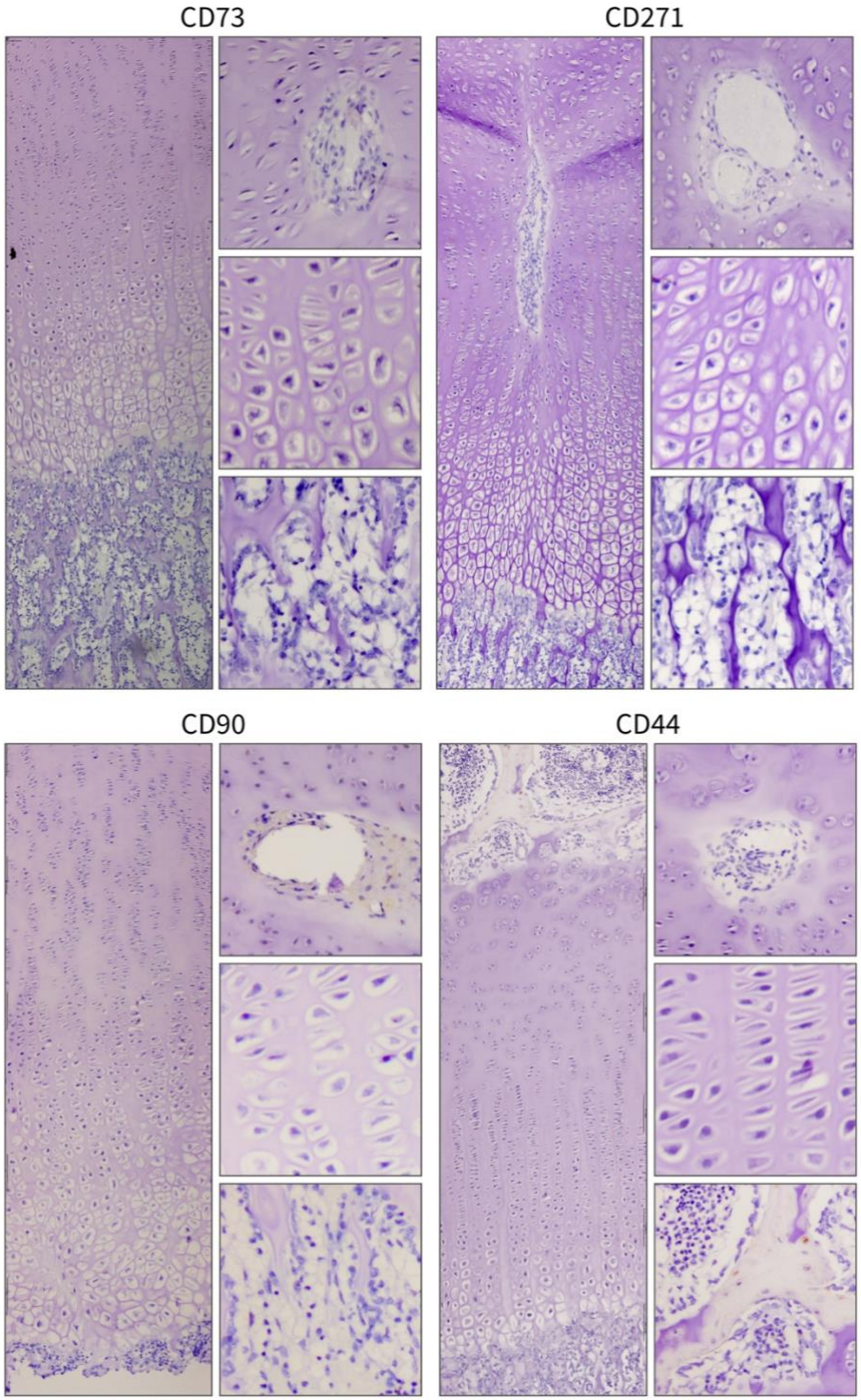

Figure 5: Qualification of CD-marker expression in the porcine growth plate. The left pictures provide an overview if expression throughout the growth plate. The right images provide a zoomed in view of the resting zone, hypertrophic zone, and of the bone fraction. Immunohistochemical staining of surface markers CD73, CD271, CD90, and CD44 is shown.

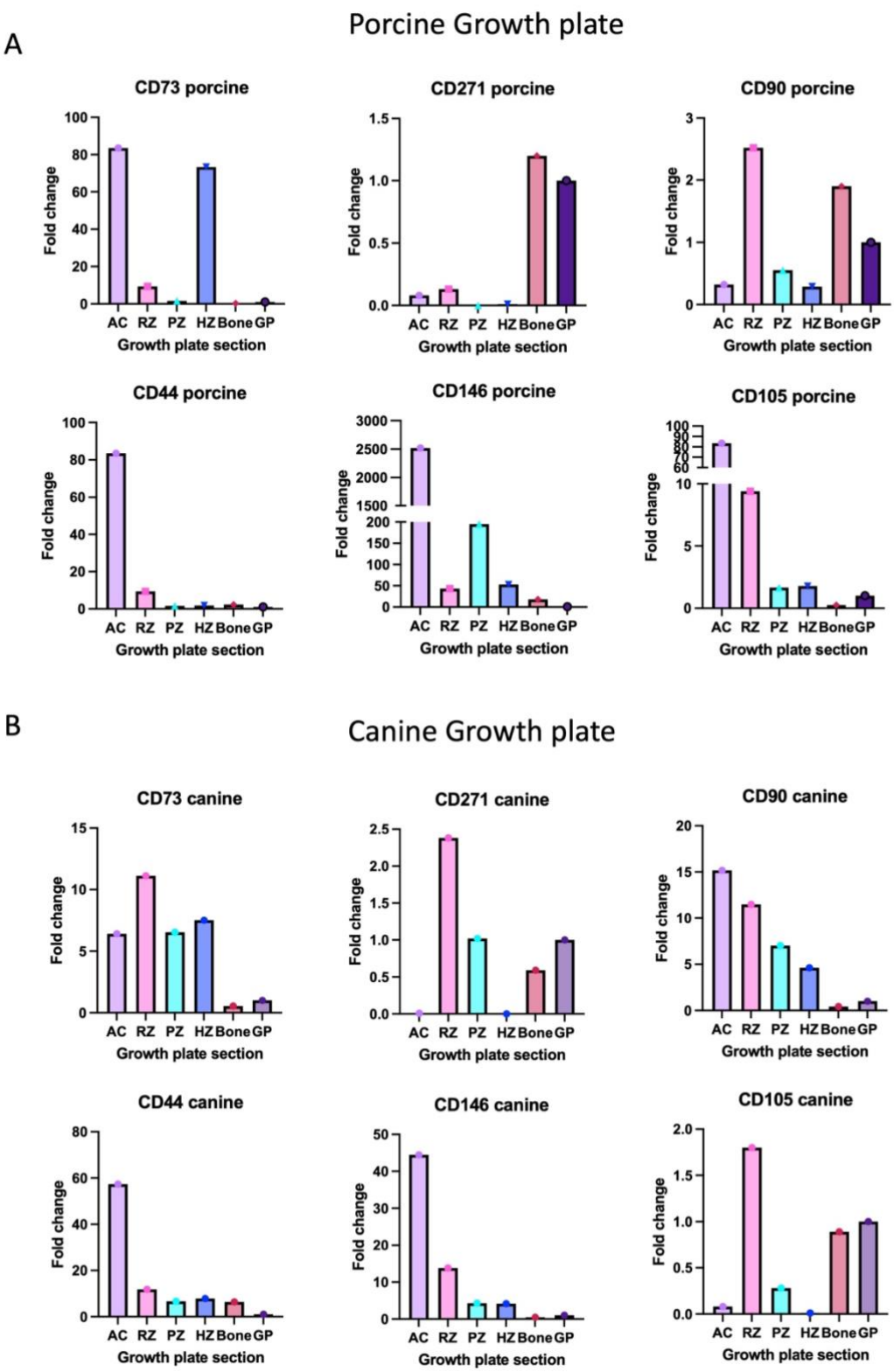

Figure 4: Relative gene expression of surface markers in the specific zones of the growth plate. RT-qPCR results for CD73, CD271, CD90, CD44, CD146, and CD105. $\Delta\Delta$Ct method is used by comparing gene expression with 4 reference genes and to a pooled sample containing all zone fractions. A) relative expression of CD-markers in the porcine growth plate and B) in the canine growth plate. Broken axes are indicated with a double line break. Y-axis displays the Fold change and the X-axis the different growth plate zones.

3.4: Discussion and concluding remarks

Roughly half of the world population experiences musculoskeletal diseases like lower back pain, osteoarthritis, or a large bone defect as a result of trauma [74]. Current treatment options are not curative in most cases, highlighting the need for new regenerative approaches targeting cartilage and bone. The process of endochondral bone formation in the growth plate is the perfect *in vivo* template to study the formation of cartilage and bone. At this moment, there is a need for an accurate *in vitro* model of the growth plate to reduce the need for laboratory animals and provide the possibility for personalized medicine approaches.

This project focused on creating an *in vitro* model using primary cells from species that resemble the human process of endochondral ossification in the growth plate: dogs and pigs. The first challenge was to isolate primary growth plate cells (GPCs) from a canine cadaver and culture this in similar conditions as the ATDC5 cells in **Chapter 2**. This is done to determine if primary GPCs respond in a similar manner to the culture conditions as the cell line. GAGs and collagen type II were produced in a similar pattern compared with the ATDC5 spheroids, although the distribution was different. In the primary cell micro-aggregates, GAGs and collagen type II were dispersed throughout the entire micro-aggregate, except for a small outlining rim of cells. This uniform distribution of GAGs and collagen type II suggests that most of the primary GPCs show chondrogenic differentiation.

Another interesting finding is that the dog GPC micro-aggregates produce collagen type I-rich matrix. This is not seen in the ATDC5 micro-aggregates in **Chapter 2**, but this difference can be easily explained. The primary GPCs consist of a pool of cells from the entire growth plate. This includes progenitor cells but also more matured chondrocytes and a small piece of bone fraction. The osteoblasts that reside in the bone fraction are known to produce large amounts of collagen type I which explains the expression in the micro-aggregates [70]. Another explanation for collagen type I production could be that cells dedifferentiated to a fibroblast-like phenotype [94–96]. These cells are capable of collagen type I production as well. For future reference, analysis of osteoblast markers like alkaline phosphatase (ALP) and osteocalcin (OCN) could conclude which of the two cell types is responsible for the production of collagen type I-rich matrix [97].

Keeping in mind that the primary GPCs consist of a pool of cells from all stages of chondrogenic maturation, it is somewhat surprising that no collagen type X was produced by the primary cell micro-aggregates. If the previously discussed theory is true, then it would be suspected that the cell fraction contains hypertrophic chondrocytes that should, in theory, be able to produce a collagen type X-rich matrix. Nonetheless, primary cells are difficult to work with. The cells often fail to adhere and proliferate and have a finite lifespan [98,99]. Because the primary cells were first cultured in monolayer until P1 before seeding them in 3D culture, it could be that the hypertrophic chondrocytes failed to attach and proliferate while resting and proliferative zone chondrocytes did expand. This would mean that the hypertrophic chondrocytes are not present in the heterogenous cell population in the micro-aggregates which would be an explanation for the lack of collagen X in the matrix. Another plausible explanation for this is that the primary chondrocytes dedifferentiated to fibroblasts before the 3D culture. Chondrocytes are likely to dedifferentiate in monolayer culture when not properly stimulated, or when the cell population is not dense enough [94]. Due to the low cell yield and proliferation rate of primary GPCs, the latter is plausible to have happened. Next, it could also be possible that the primary dog GPCs do not respond in the same way to BMP-4 as the ATDC5 cells do and that there are different factors needed to drive hypertrophy in the primary micro-aggregates.

The aim of the 3D culture experiment with primary GPCs was to see if these cells could be isolated, expanded, and differentiated towards the chondrogenic lineage. As shown, the use of a

heterogeneous pool of GPCs has an impact on the process of endochondral bone formation in the micro-aggregate because these cells are not properly structured. A solution for this would be to use the reserve zone progenitor cells in a 3D *in vitro* culture model. These cells contain the correct factors to drive chondrogenic maturation in a structured manner as seen in the growth plate *in vivo*. The use of these cells would make for a more realistic, translational, and structured *in vitro* model. Therefore, the second aim of this chapter was to identify the resting zone progenitor cells using the markers: CD90, CD44, CD73, CD271, CD105, and CD146.

Immunohistochemical analysis revealed the localisation of the surface markers CD271, CD44, CD73, and CD90 in the canine and porcine growth plate. A few differences in localisation were observed between the two species regarding CD44 and CD271. CD73 and CD44 showed no positive staining in the resting zone of both species, whereas CD90 did. CD271 only showed presence in the canine resting zone and not in the porcine resting zone. This difference between canine and porcine tissue could be explained by the species reactivity of the primary antibodies used for immunohistochemical analysis even though no further testing is performed to confirm this. Species reactivity should be confirmed in the future to determine the presence of these surface markers in porcine as is already established in the canine growth plate. The absence of CD73 in the resting zone of the growth plate renders this marker a possible negative marker that could be used to filter out non-progenitor cells. Since CD73 does show clear presence in the proliferative zone of the growth plate, this marker shows potential in separating the resting and proliferative zone. This is likely the most difficult separation to make due to the small differences between these zones [11,12]. Furthermore, the MSC markers CD271, CD90, and CD44 were present in the resting zone of the growth plate, meaning that these markers are possible positive targets for cell sorting. While MSCs lack a clearly defined surface marker profile, they present an array of surface markers that provide clues for proliferation and differentiation capacity [100]. CD271, CD105, and CD146 are for example surface antigens that have been reported as predictive markers for chondrogenic differentiation potential [101–103]. To further specify markers for chondrogenic differentiation potential, Cicione *et al*, 2010 established CD29 as a surface marker indicative of high chondrogenic potential [104]. Furthermore, MSCs need to show negative expression for the markers CD45, CD34, CD14, CD79 or CD19 for correct characterisation [105]. CD271 and CD90 pose as potential surface markers for identifying growth plate progenitor cells. It is likely beneficial to supplement these markers with CD146 and CD105 and maybe CD29 to achieve a higher specificity for the isolation of progenitor cells. furthermore, CD73 and other negative MSC markers like CD45 and CD34 could pose as negative markers during cell sorting. An interesting point of discussion is however that the markers presented by MSCs are established *in vitro*. Several studies have already revealed that the expression of surface markers changes as a result of *in vitro* culturing [104,106–108]. This could mean that the MSC descending resting zone progenitor cells might display a different set of surface markers *in vivo*.

The presence of the surface markers, including CD105 and CD146, in the resting zone was analysed through RT-qPCR which required separation of the different zones of the growth plate for zone-specific gene expression analysis. Correct separation of the porcine growth plate was validated using expression analysis of chondrogenic genes expressed by chondrocytes in different stages of maturation. *COL10A1* is expressed the highest in the hypertrophic zone of the growth plate which is confirmed in the porcine growth plate. *SFRP5* exhibits a good opportunity to determine correct separation of the resting zone since this gene is known to be expressed in the resting zone. Therefore, all the genes confirmed correct separation of the growth plate zones in the porcine growth plate. On the contrary, this was not the case in the canine growth plate in which, *COL10A1* was expressed in all three growth plate zones. Furthermore, *COL1A1* was expressed the highest in the resting zone. The first could be explained by the size of the growth plate. The growth plates of the large bones in the legs of a stillborn pup were used. The growth plates were very small which made correct dissection extremely difficult with a scalpel blade. The latter, also a result of the size of the growth plate, could be explained by the remaining periosteum in the resting zone fraction. In the

future, better dissection of the growth plate can be achieved by using larger growth plates or by using laser capture microdissection to separate the different zones of very small growth plates [85,109]. Nonetheless, the porcine zones can give us information on the presence of the surface markers in the resting zone fraction.

The expression of the surface markers *CD44, CD90, CD73, CD271, CD105,* and *CD146* in the resting zone was confirmed in both the canine and the porcine growth plates. However, the results of the canine growth plate were limited due to incorrect dissection of the different growth plate zones for gene expression analysis. The low expression of CD271 in the resting zone fraction is in line with the IHC staining. CD90 and CD44 show a correlation between the qualitative staining of the marker and the relative gene expression. CD73 on the contrary, did not show positive staining in the growth plate resting zone, but does show an increased expression of the marker. Upregulated gene expression does not necessarily correlate with protein surface expression, but it could be an indication that CD73 is indeed present in the resting zone of the growth plate. Although gene expression is not necessarily correlated with surface marker expression, this is still an indication that CD73 might not be the best marker to use as a negative selection marker. Previously, a skeletal stem cell marker set was established by Wu *et al*, 2017 [86]. This study revealed CD146 and CD105 as potential markers for the isolation of resting zone progenitors. Both the CD146 and the CD105 positive populations confirmed proliferation capacity and chondrogenic differentiation potential of the isolated cells. The relative gene expression of CD146 and CD105 confirm that there is a presence of these markers in the resting zone. However, immunohistochemical staining of these markers could give more insight in the exact localisation. For now, CD146, CD105, CD271, and CD90 appear to be the most promising candidates for isolating the progenitor cells out of the resting zone. A step that could be taken in improving the specificity of the cell sorting, is minimizing bone tissue present in the cell fraction. Bone marrow especially contains a lot of MSCs, also from different lineages, which increases the difficulty in reaching a pure progenitor population [110].

To conclude the results displayed in this chapter, primary dog GPCs can be isolated and cultured as a heterogenous population and produce GAGs, collagen type II, and type I production in an *in vitro* 3D culture model. However, collagen X was not produced by these cells. Furthermore, markers CD146, CD105, CD90, and CD271 seem to be promising to isolate reserve zone cells. Future work should be focused on further identifying and isolating the progenitor cell fraction via FACS cell sorting by focusing on CD146, CD105, CD271, and CD90 as potential surface markers. A colony-forming assay can confirm proliferation potential, and chondrogenic differentiation potential can be assessed with multi-lineage differentiation assays. Furthermore, the MSC population that form the resting zone progenitor population is already committed to the chondrogenic lineage. Validating if the progenitor fraction can be stimulated towards other lineages apart from the chondrogenic lineage could provide crucial information on the specificity of the progenitor cell isolation. In conclusion, this study has shown progress in creating an *in vitro* model of the epiphyseal growth plate and highlights the identification of promising surface markers to identify the resting zone progenitor cells, paving the way for more effective strategies in bone regeneration in the future.

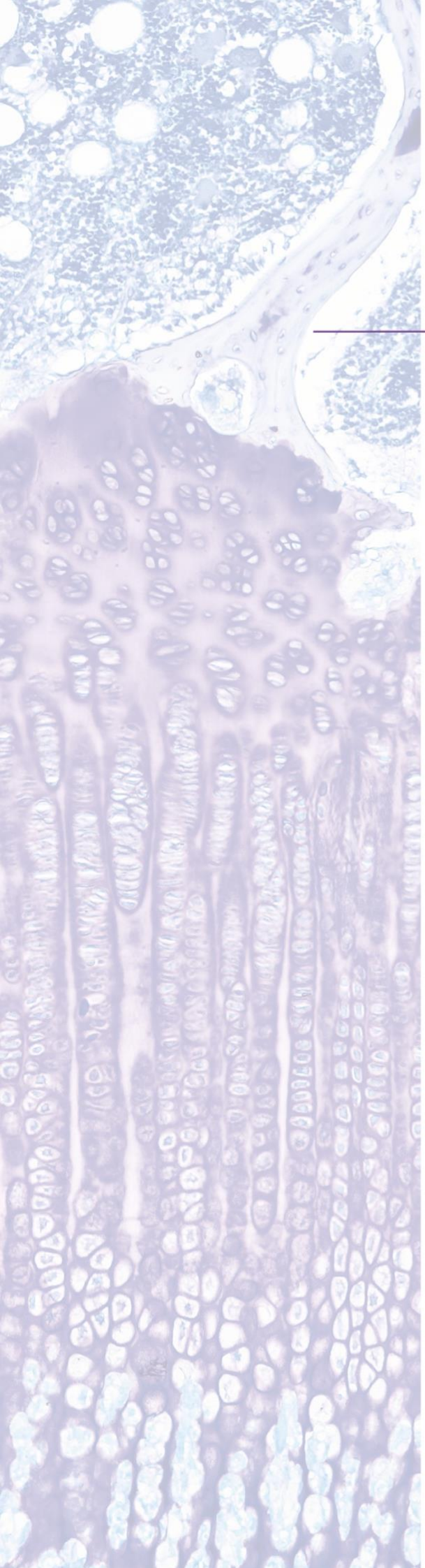

Chapter 4

General discussion and concluding remarks

Current regenerative strategies targeting cartilage and bone often fail due to the harsh hypoxic environment of the cartilage [13]. For the treatment of for example large bone defects, such strategies are necessary for developing a curative treatment. The process of endochondral ossification in the growth plate supplies an excellent template for studying cartilage and bone generation *in vivo*.

The overall aim of this thesis was to make studying the process of endochondral bone formation more accessible and controllable via the development of a 3D *in vitro* model of the growth plate. This was attempted utilizing the ATDC5 cell line and primary growth plate cells of canine and porcine origin. The ATDC5 cell line was used because it is easy to work with, widely available, and this cell line has the potential for chondrogenic differentiation *in vitro* [45]. Furthermore, the ATDC5 cell line could easily be used to identify a promising media composition and to optimize the culture condition to achieve the goal. Ultimately, the overall goal is to develop an accurate, easy to access *in vitro* model of the growth plate. This requires a different cell type to model the growth plate because the ATDC5 cell line is mouse derived. It is known that the growth plate of mice does not close upon maturation while this is the case in most mammals, including humans [11,29,40,73]. On top of that, the ATDC5 cell line is an immortalized cell line, meaning that the cells have been manipulated to proliferate indefinitely [72]. Due to these modifications, including the expression of specific genes, these cells cannot be considered as representative of the *in vivo* situation [72]. However, the use of a continuous cell line also has advantages which are very good for optimizing a culture system. First of all, because the cell population is homogenous and generates consistent results. Secondly, the cell line is easy to culture and does not require extraction from a living animal which results in a larger availability of cells. This shows the advantages of using the ATDC5 cell line for optimisation purposes but also stresses the importance of continuing the work with primary growth plate cells of a species closer to humans.

To develop a representative *in vitro* growth plate model, cells derived from the target species itself, or from species that resemble the human situation are needed. Dogs are such species in which the growth plate closes upon maturation and shows similar characteristics compared to the human growth plate. In addition, bone defects are also common in dog patients and therefore they are the target species as well. This is why in **Chapter 3** primary dog GPCs are isolated from canine growth plates and cultured in a 3D culture model. In this case, a similar composition of the differentiation medium, as well as similar culture conditions to the ATDC5 micro-aggregates cultured in **Chapter 2** are used. This is done to validate if the primary GPCs need the same culture conditions to reach their potential for endochondral ossification as the immortal ATDC5 cell line. Both cell types were cultured for 21 days in a normoxic environment with differentiation media supplemented with 50 ng/mL TGF-β or 50 ng/mL BMP-4. Both cell types produce a matrix rich in GAGs and collagen II when stimulated with TGF-β, however, the matrix is spread more uniformly in the dog GPC micro-aggregates, whereas the matrix in the ATDC5 micro-aggregates is produced more in the periphery but not in the centre of the aggregates. As mentioned before, this might be due to the presence of already differentiated chondrocytes in the dog GPCs. The cell population is very heterogenous and descends directly from the growth plate. BMP-4 induced GAG and collagen type II rich matrix production in both cell types as well. The main difference between the cultures with the two cell types is that the ATDC5 aggregates could be driven to produce collagen X whilst this is not the case in the primary dog GPCs. However, dog GPCs were never cultured with TGF-β with subsequential BMP-4 stimulation, which is the condition that resulted in the best chondrogenic differentiation in the ATDC5 cell line. To conclude whether the dog GPCs are driven to chondrogenic differentiation is hard. The primary micro-aggregates express collagen type I and do not express collagen type X which is in contrast to what is seen in the ATDC5 micro-aggregates. The expression pattern of the primary micro-aggregates could be the result of dedifferentiated chondrocytes toward a fibroblast-like phenotype. This would mean that the stimulation with TGF-β or BMP-4 is not sufficient in driving hypertrophic differentiation of the primary dog GPCs. Further experiments to confirm if dedifferentiation occurred

have to be conducted, before continuing with achieving chondrogenic differentiation in the primary cells.

The overall chondrogenic differentiation achieved, both in the ATDC5 and in the primary dog GPC micro-aggregates, leaves room for improvement. This thesis covers stimulation of the first stage in chondrogenic differentiation with TGF-β and aims to stimulate hypertrophic differentiation with BMP-4. First of all, culturing the micro-aggregates over a longer period, like 28 or 35 days will be interesting to see how the production of collagen type X and maybe even collagen type 1 develops. However, TGF-β and BMP-4 are not the only factors involved in chondrogenic maturation. BMPs form an interesting gradient of agonists and antagonists through the growth plate in which antagonists like BMP-7 are expressed in the resting zone and agonists like BMP-4, 6 and 2 in the hypertrophic zone [16,69]. Combining TGF-β with BMP-7 during the first week(s) of stimulation followed by subsequential BMP-2, 4, or 6 stimulation can be an interesting combination to achieve better chondrogenic differentiation. Furthermore, An *et al*, 2010 revealed that human insulin growth like factor 1 (IGF-1) can also have a role in inducing matrix production supplementary to TGF-β and BMP-7 [111]. The fibroblast growth factor (FGF) family, specifically FGF-2, is also known to induce chondrogenic differentiation, especially proliferation and GAG production [112]. Several factors could be added in order to optimize chondrogenic differentiation *in vitro* to create the most accurate growth plate model [113]. In conclusion, the pursuit of enhanced chondrogenic differentiation demands further exploration through extended culture periods, potential synergistic combinations of TGF-β, BMPs, and other growth factors, which offers potential in refining the 3D *in vitro* model of the growth plate.

Unfortunately, the heterogenous growth plate cell population is not the most representative of the processes occurring in the growth plate. In future culture models, it would be ideal to culture a 3D model *in vitro* using the progenitor cells located in the resting zone since these cells are capable of replenishing the growth plate and contain the correct factors to drive chondrogenic maturation and differentiation in a more organised manner. To achieve this, a marker set to identify and isolate these cells has to be developed. In **chapter 3** several markers are analysed for their presence and expression in the resting zone of the growth plate. CD271, CD90, CD146, and CD105 displayed expression in the resting zone of the growth plate which renders these potential positive markers to use for cell sorting. CD73 is a MSC marker known to predict chondrogenic differentiation, however, due to the negative immunohistochemical staining in the growth plate, this marker will be left out of the consideration until presence in the resting zone can be confirmed. Furthermore, CD73 is likely present on already further differentiated chondrogenic cells, rendering this not the correct marker to identify the progenitors [114]. To increase specificity, a more specific marker for chondrogenic differentiation like CD29 could be explored. This can be combined with using negative MSC markers like CD45 and CD34 to further specify the the progenitor cell fraction. Further work needs to be conducted to confirm the stemness of this population by determining the proliferation and differentiation potential of the isolated cells before these cells would be suitable to use in a 3D *in vitro* culture model of the growth plate.

The work discussed so far solely focuses on achieving chondrogenic differentiation *in vitro*. However, to model endochondral bone formation, it is essential to simulate the remodelling of the cartilage template into bone *in vitro* as well. A major limitation in this pursuit is the lack of perfusion and influx of osteogenic cells. An intriguing future advancement for the model entails the incorporation of perfusion. The circulatory network, specifically the blood vessels, is an important and prominent component of the resting zone within the growth plate. These vessels play a vital role in sustaining the stem cell niche and delivering essential factors required for driving chondrogenic maturation. Presently, the existing in vitro model lacks the capability of perfusion. However, the development of a growth plate-on-a-chip model could represent an exciting step forward in modelling the growth

plate. In this envisioned setup, resting zone progenitor cells could be cultured in close proximity to resting zone endothelial cells, which hold the potential to provide the progenitors with the necessary factors. Such an approach has the potential to eliminate the necessity for manually stimulating the cells with growth factors to induce chondrogenic maturation. This renders the growth plate-on-a-chip model a very promising approach for reaching a translational *in vitro* representation of the growth plate and thereby allowing new research into endochondral ossification.

The use of the resting zone progenitor cells rather than the ATDC5 cell line and primary growth plate cells has several advantages. For example, in studying intra-species height differences. Differences in adult height are the result genetic variations that affect the process of endochondral bone formation. These variations can impact the regulation in each of the distinct growth plate zones. A taller stature, for example, is paired with a larger hypertrophic zone and a faster proliferation rate compared to people with a short stature [81,82,115]. Investigating the physiological differences in growth plate regulation could provide insight into how chondrocytes transition through different stages of maturation and how this process can be manipulated to achieve bone regeneration. The use of resting zone progenitor cells in an *in vitro* model of the growth plate allows for the use of species-specific progenitors. This means that different models could be obtained for small-breed dogs like the Pomeranian and large-breed dogs like the Great Dane. Modelling these species *in vitro* could be a game-changer in studying the process of endochondral bone formation and identifying new targets for the development of novel regenerative therapies. Furthermore, the possibilities of modifying these *in vitro* models are nearly endless meaning that studying endochondral ossification could be changed forever.

Furthermore, progenitor cells from humans could be used for *in vitro* modelling as well to study the human growth plate directly. The material could be obtained from growth plate corrective surgery [116]. This would increase the translatability of findings to the human growth plate greatly. Ultimately, the development of an accurate *in vitro* model of the growth plate will increase knowledge on processes occurring during endochondral ossification, but could also provide a platform to study pathways linked to growth disorders or the progression of musculoskeletal disease [13]. This knowledge can be used to develop new treatment strategies for musculoskeletal tissues like cartilage and bone. Hopefully, this knowledge will lead to improved quality of life for millions of animals and humans worldwide.

The development of an *in vitro* model is an important way to replace animal models, thus reducing the need for animal sacrifice. Regarding this, using the resting zone progenitor cells still use animal tissue that often requires animal sacrifice. This is also a limiting factor in the availability of growth plate tissue. Another cell source that surpasses these limitations are induced pluripotent stem cells (iPSCs). iPSCs are adult cells that are reprogrammed into pluripotent stem cells with the use of reprogramming factors like Sox2, Oct4, Nanog, c-Myc and Klf4 (**Figure 1**) [117]. iPSCs regain stemness and can be differentiated again into different lineages, including the chondrogenic lineage. The main advantage of using these cells is that a skin biopsy is sufficient to retrieve iPSCs, meaning that no animal sacrifice is needed to obtain the required tissue. On top of that, similar to the progenitor cells, the iPSCs can not only be used for species-specific modelling of the growth plate but also patient-specific modelling.

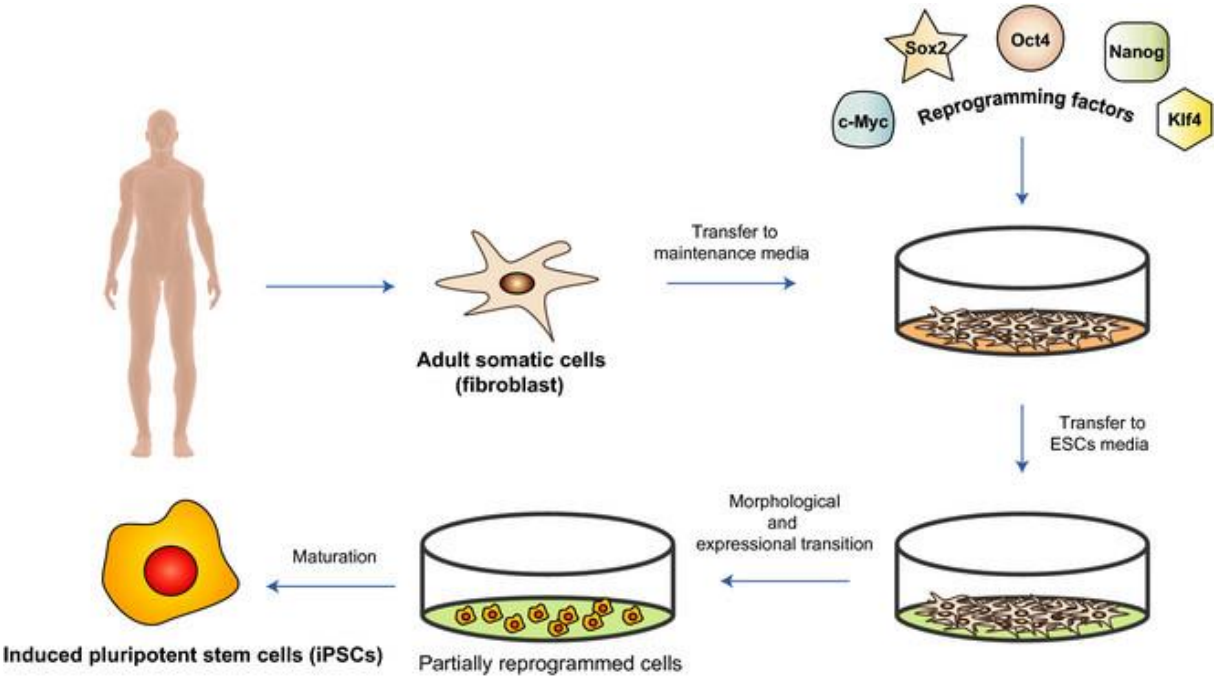

Figure 1: Overview of how adult cells obtained from a biopsy are reprogrammed to induced pluripotent stem cells. Figure obtained from Rony et al, 2015 [117]

Several studies have already been conducted in which iPSCs are stimulated towards hypertrophic chondrocytes *in vitro.* Kamakura *et al*, 2023 achieved hypertrophic chondrocytes by stimulating human iPSCs towards sclerotome first followed by culturing these cells in a differentiation medium supplemented with TGF-β3 and BMP-4 [118]. The resulting pellets can produce GAGs, collagen II, and collagen X, suggesting chondrogenic maturation. Similarly, Zhang *et al,* 2020 studied the development of cartilage and bone by stimulating iPSCs with FGF-2 and BMP-4 [119]. These cell pellets were able to regenerate cartilage within 28 days of culture. Lamandé *et al,* 2023 modelled skeletal development *in vitro* using human iPSCs and even reached chondrocyte transition into osteoblasts and remodelling into bone [37]. Thus far, iPSCs appear to be the current most promising cell source for modelling endochondral ossification *in vitro*. Nevertheless, iPSCs encounter a lot of limitations concerning the reproducibility, batch-to-batch variability, reprogramming efficiency, and accessibility. First of all, reprogramming adult cells to pluripotent stem cells is a very inefficient process. Adult somatic cells have to overcome many barriers before reaching pluripotency, which results in only a small amount of cells actually reaching this stage [120]. Furthermore, due to the diverse genetic backgrounds of different donors, there is a large variability in iPSC batches [121]. As mentioned before, one of the causes for which the 3D *in vitro* model of the growth plate can be utilized is to study intra-species height differences. Batch-to-batch variation is an important factor of which the impact has to be further investigated to make sure that these variations do not overshadow the intra-species differences. In summary, while significant progress has been made in driving iPSCs towards hypertrophic chondrocytes and modelling endochondral ossification, challenges relating to reprogramming efficiency, batch-to-batch variability, and reproducibility have to be addressed to fully grasp the potential of iPSCs for creating a 3D *in vitro* growth plate model.

To conclude, the journey towards a comprehensive understanding of endochondral ossification and the development of an accurate *in vitro* model of the growth plate is marked by noteworthy accomplishments as well as exciting potential for future improvements. The goal of reaching enhanced chondrogenic differentiation remains a central focus, in which prolonged culture durations and synergistic combinations of important factors like TGF-β and BMPs are key in future developments. The complicated interaction of BMP gradients and the potential involvement of

growth factors like IGF-1 and FGF-2 offer interesting opportunities for future research on unravelling the complex nature of the growth plate. The use of species-specific resting zone progenitor cells shows potential in providing a more translatable variant of the *in vitro* model. Furthermore, the proposed growth plate-on-a-chip model offers a positive outlook for addressing the growth plate model's perfusion limitations in an approach to breach the step towards remodelling the cartilage template into bone. The sum of these studies together has the potential to not only increase our understanding of endochondral bone formation, but also to improve research into underlying mechanisms of growth disorders, musculoskeletal diseases, and novel regenerative strategies, all to ultimately improve the quality of life for both animals and humans on a global scale.

Literature

1. Migliorini, F. *et al.* Strategies for large bone defect reconstruction after trauma, infections or tumour excision: a comprehensive review of the literature. *Eur. J. Med. Res.* **26**, (2021).
2. Ghoneimy, A. M. El, Sherbiny, M. El & Kamal, N. Use of Vascularized Fibular Free Flap in the Reconstruction of the Femur in Pediatric and Adolescent Bone Sarcomas: Complications and Functional Outcome. *J. Reconstr. Microsurg.* **35**, 156–162 (2019).
3. Mankin, H. J., Hornicek, F. J. & Raskin, K. A. Infection in massive bone allografts. *Clin. Orthop. Relat. Res.* **432**, 210–216 (2005).
4. Hinsenkamp, M. *et al.* Adverse reactions and events related to musculoskeletal allografts: Reviewed by the World Health Organisation Project NOTIFY. *Int. Orthop.* **36**, 633–641 (2012).
5. Fung, B., Hoit, G., Schemitsch, E., Godbout, C. & Nauth, A. The induced membrane technique for the management of long bone defects. *Bone Jt. J.* **102**, 1723–1734 (2020).
6. Villemagne, T. *et al.* Intercalary segmental reconstruction of long bones after malignant bone tumor resection using primary methyl methacrylate cement spacer interposition and secondary bone grafting: The induced membrane technique. *J. Pediatr. Orthop.* **31**, 570–576 (2011).
7. Baek, I. *et al.* Therapeutic potential of epiphyseal growth plate cells for bone regeneration in an osteoporosis model. *J. Tissue Eng.* **13**, (2022).
8. C., N. & Varela-Nallar, L. Bone and Cartilage Regeneration: Wnt Signaling Pathway in Healing. *Trends Cell Signal. Pathways Neuronal Fate Decis.* (2014). doi:10.5772/54606
9. Van Der Eerden, B. C. J., Karperien, M. & Wit, J. M. Systemic and Local Regulation of the Growth Plate. *Endocrine Reviews* **24**, 782–801 (2003).
10. Lui, J. C., Nilsson, O. & Baron, J. Recent Insights into the Regulation of the Growth Plate. *J. Mol. Endocrinol.* **53**, T1 (2014).
11. Ağirdil, Y. The growth plate: A physiologic overview. *EFORT Open Rev.* **5**, 498–507 (2020).
12. Burdan, F. *et al.* Morphology and physiology of the epiphyseal growth plate. *Folia Histochem. Cytobiol.* **47**, 5–16 (2009).
13. Tiffany, A. S. & Harley, B. A. C. Growing Pains: The Need for Engineered Platforms to Study Growth Plate Biology. *Adv. Healthc. Mater.* **11**, 2200471 (2022).
14. Karimian, E., Chagin, A. S. & Sävendahl, L. Genetic Regulation of the Growth Plate. *Front. Endocrinol. (Lausanne).* **2**, (2011).
15. Horton, W. A., Hall, J. G. & Hecht, J. T. Achondroplasia. *Lancet* **370**, 162–172 (2007).
16. Garrison, P., Yue, S., Hanson, J., Baron, J. & Lui, J. C. Spatial regulation of bone morphogenetic proteins (BMPs) in postnatal articular and growth plate cartilage. *PLoS One* **12**, e0176752 (2017).
17. De Luca, F. *et al.* Regulation of growth plate chondrogenesis by bone morphogenetic protein-2. *Endocrinology* **142**, 430–436 (2001).
18. Kobayashi, T., Lyons, K. M., McMahon, A. P. & Kronenberg, H. M. BMP signaling stimulates cellular differentiation at multiple steps during cartilage development. *Proc. Natl. Acad. Sci. U. S. A.* **102**, 18023–18027 (2005).
19. Anderson, H. C., Hodges, P. T., Aguilera, X. M., Missana, L. & Moylan, P. E. Bone Morphogenetic Protein (BMP) Localization in Developing Human and Rat Growth

Plate, Metaphysis, Epiphysis, and Articular Cartilage. *J. Histochem. Cytochem.* **48**, 1493–1502 (2000).
20. Shum, L., Wang, X., Kane, A. A. & Nuckolls, G. H. BMP4 promotes chondrocyte proliferation and hypertrophy in the endochondral cranial base. *Int. J. Dev. Biol.* **47**, 423–431 (2003).
21. Wu, M., Chen, G. & Li, Y. P. TGF-β and BMP signaling in osteoblast, skeletal development, and bone formation, homeostasis and disease. *Bone Res.* **4**, (2016).
22. Wang, W., Rigueur, D. & Lyons, K. M. TGFβ as a gatekeeper of BMP action in the developing growth plate. *Bone* **137**, 115439 (2020).
23. Samsa, W. E., Zhou, X. & Zhou, G. Signaling Pathways Regulating Cartilage Growth Plate Formation and Activity. *Semin. Cell Dev. Biol.* **62**, 3 (2017).
24. Dy, P. *et al.* Sox9 Directs Hypertrophic Maturation and Blocks Osteoblast Differentiation of Growth Plate Chondrocytes. *Dev. Cell* **22**, 597 (2012).
25. Caron, M. M. J. *et al.* Hypertrophic differentiation during chondrogenic differentiation of progenitor cells is stimulated by BMP-2 but suppressed by BMP-7. *Osteoarthr. Cartil.* **21**, 604–613 (2013).
26. Haseeb, A. *et al.* SOX9 keeps growth plates and articular cartilage healthy by inhibiting chondrocyte dedifferentiation/ osteoblastic redifferentiation. *Proc. Natl. Acad. Sci. U. S. A.* **118**, e2019152118 (2021).
27. Zieba, J. T., Chen, Y. T., Lee, B. H. & Bae, Y. Notch Signaling in Skeletal Development, Homeostasis and Pathogenesis. *Biomolecules* **10**, (2020).
28. McGovern, J. A., Griffin, M. & Hutmacher, D. W. Animal models for bone tissue engineering and modelling disease. *Dis. Model. Mech.* **11**, (2018).
29. Börjesson, A. E. *et al.* The role of estrogen receptor-α and its activation function-1 for growth plate closure in female mice. *Am. J. Physiol. - Endocrinol. Metab.* **302**, E1381 (2012).
30. Oviawe, E. I., Yakubu, A. S., Kene, R. & Shehu, S. A. Radiographic Evaluation of the Appearance and Closure Time of Growth Plates of Radius and Ulna Bones in Nigerian Indigenous Dogs. *J Vet Ani Res* **1**, 101 (2018).
31. Raimann, A., Javanmardi, A., Egerbacher, M. & Haeusler, G. A journey through growth plates: tracking differences in morphology and regulation between the spine and the long bones in a pig model. *Spine J.* **17**, 1674–1684 (2017).
32. Hartung, T. Thoughts on limitations of animal models. *Parkinsonism Relat. Disord.* **14**, S81–S83 (2008).
33. Hubrecht, R. C. & Carter, E. The 3Rs and Humane Experimental Technique: Implementing Change. *Anim. an Open Access J. from MDPI* **9**, (2019).
34. van Gool, S. A. *et al.* Fetal Mesenchymal Stromal Cells Differentiating towards Chondrocytes Acquire a Gene Expression Profile Resembling Human Growth Plate Cartilage. *PLoS One* **7**, (2012).
35. Randall, R. M., Shao, Y. Y., Wang, L. & Ballock, R. T. Activation of Wnt Planar cell polarity (PCP) signaling promotes growth plate column formation in vitro. *J. Orthop. Res.* **30**, 1906–1914 (2012).
36. Watts, A. E., Ackerman-Yost, J. C. & Nixon, A. J. A comparison of three-dimensional culture systems to evaluate in vitro chondrogenesis of equine bone marrow-derived mesenchymal stem cells. *Tissue Eng. Part A* **19**, 2275–2283 (2013).
37. Lamandé, S. R. *et al.* Modeling human skeletal development using human pluripotent stem cells. *Proc. Natl. Acad. Sci. U. S. A.* **120**, e2211510120 (2023).

38. Mackie, E. J., Ahmed, Y. A., Tatarczuch, L., Chen, K. S. & Mirams, M. Endochondral ossification: How cartilage is converted into bone in the developing skeleton. *Int. J. Biochem. Cell Biol.* **40**, 46–62 (2008).
39. Sananta, P., Isnansyah, Y., Rosandi, R. D. & Sugiarto, M. A. The Management Growth Plate Injury in Animal Studies with Stem Cells Technique: Systematic Review. *Acta Inform. Medica* **30**, 53 (2022).
40. Kilborn, S. H., Trudel, G. & Uhthoff, H. Review of Growth Plate Closure Compared with Age at Sexual Maturity and Lifespan in Laboratory Animals.
41. King, T. A. The One Medicine concept: its emergence from history as a systematic approach to re-integrate human and veterinary medicine. *Emerg. Top. Life Sci.* **5**, 643 (2021).
42. Burdick, J. A. & Vunjak-Novakovic, G. Engineered microenvironments for controlled stem cell differentiation. *Tissue Eng. - Part A* **15**, 205–219 (2009).
43. Duval, K. *et al.* Modeling Physiological Events in 2D vs. 3D Cell Culture. *Physiology* **32**, 266 (2017).
44. Baker, B. M. & Chen, C. S. Deconstructing the third dimension-how 3D culture microenvironments alter cellular cues. *J. Cell Sci.* **125**, 3015–3024 (2012).
45. Yao, Y. & Wang, Y. ATDC5: an excellent in vitro model cell line for skeletal development. *J. Cell. Biochem.* **114**, 1223–1229 (2013).
46. Tare, R. S., Howard, D., Pound, J. C., Roach, H. I. & Oreffo, R. O. C. Tissue engineering strategies for cartilage generation—Micromass and three dimensional cultures using human chondrocytes and a continuous cell line. *Biochem. Biophys. Res. Commun.* **333**, 609–621 (2005).
47. Le, B. Q., van Blitterswijk, C. & de Boer, J. An Approach to In Vitro Manufacturing of Hypertrophic Cartilage Matrix for Bone Repair. *Bioeng. 2017, Vol. 4, Page 35* **4**, 35 (2017).
48. Kim, J., Tomida, K., Matsumoto, T. & Adachi, T. Spheroid culture for chondrocytes triggers the initial stage of endochondral ossification. *Biotechnol. Bioeng.* (2022). doi:10.1002/bit.28203
49. Weiss, H. E., Roberts, S. J., Schrooten, J. & Luyten, F. P. A semi-autonomous model of endochondral ossification for developmental tissue engineering. *Tissue Eng. - Part A* **18**, 1334–1343 (2012).
50. Kim, J., Tomida, K., Matsumoto, T. & Adachi, T. Spheroid culture for chondrocytes triggers the initial stage of endochondral ossification. *Biotechnol. Bioeng.* **119**, 3311–3318 (2022).
51. Richard, D. *et al.* Lineage-specific differences and regulatory networks governing human chondrocyte development. *Elife* **12**, 1–40 (2023).
52. Pretemer, Y. *et al.* Differentiation of Hypertrophic Chondrocytes from Human iPSCs for the In Vitro Modeling of Chondrodysplasias. *Stem Cell Reports* **16**, 610–625 (2021).
53. Temu, T. M., Wu, K. Y., Gruppuso, P. A. & Phornphutkul, C. The mechanism of ascorbic acid-induced differentiation of ATDC5 chondrogenic cells. *Am. J. Physiol. - Endocrinol. Metab.* **299**, E325 (2010).
54. Cheng, X. *et al.* Dexamethasone Exposure Accelerates Endochondral Ossification of Chick Embryos Via Angiogenesis. *Toxicol. Sci.* **149**, 167–177 (2016).
55. Hunziker, E. B. Differential effects of DEX on chondrogenesis. *Eur. Cells Mater.* **22**, 302–320 (2011).
56. Nakamura, K. *et al.* p38 Mitogen-activated protein kinase functionally contributes to

chondrogenesis induced by growth/differentiation factor-5 in ATDC5 cells. *Exp. Cell Res.* **250**, 351–363 (1999).
57. Nakajima, M., Negishi, Y., Tanaka, H. & Kawashima, K. p21Cip-1/SDI-1/WAF-1 expression via the mitogen-activated protein kinase signaling pathway in insulin-induced chondrogenic differentiation of ATDC5 cells. *Biochem. Biophys. Res. Commun.* **320**, 1069–1075 (2004).
58. Hoogendam, J. *et al.* Novel early target genes of parathyroid hormone-related peptide in chondrocytes. *Endocrinology* **147**, 3141–3152 (2006).
59. Anada, T. & Suzuki, O. Size regulation of chondrocyte spheroids using a PDMS-based cell culture chip. *J. Robot. Mechatronics* **25**, 644–649 (2013).
60. Bach, F. C. *et al.* The species-specific regenerative effects of notochordal cell-conditioned medium on chondrocyte-like cells derived from degenerated human intervertebral discs. *Eur. Cell. Mater.* **30**, 132–147 (2015).
61. Phornphutkul, C., Wu, K. Y. & Gruppuso, P. A. The role of insulin in chondrogenesis. *Mol. Cell. Endocrinol.* **249**, 107–115 (2006).
62. Yao, Y., Zhai, Z. & Wang, Y. Evaluation of Insulin Medium or Chondrogenic Medium on Proliferation and Chondrogenesis of ATDC5 Cells. *Biomed Res. Int.* **2014**, (2014).
63. Hirao, M., Tamai, N., Tsumaki, N., Yoshikawa, H. & Myoui, A. Oxygen Tension Regulates Chondrocyte Differentiation and Function during Endochondral Ossification. *J. Biol. Chem.* **281**, 31079–31092 (2006).
64. Hiraki, Y. *et al.* Identification of Chondromodulin I as a Novel Endothelial Cell Growth Inhibitor: PURIFICATION AND ITS LOCALIZATION IN THE AVASCULAR ZONE OF EPIPHYSEAL CARTILAGE. *J. Biol. Chem.* **272**, 32419–32426 (1997).
65. Lee, H. H. *et al.* Hypoxia Enhances Chondrogenesis and Prevents Terminal Differentiation through PI3K/Akt/FoxO Dependent Anti-Apoptotic Effect. *Sci. Reports 2013 31* **3**, 1–12 (2013).
66. Chen, L., Fink, T., Ebbesen, P. & Zachar, V. Hypoxic Treatment Inhibits Insulin-Induced Chondrogenesis of ATDC5 Cells Despite Upregulation of DEC1. *http://dx.doi.org/10.1080/03008200600609558* **47**, 119–123 (2009).
67. Anada, T., Fukuda, J., Sai, Y. & Suzuki, O. An oxygen-permeable spheroid culture system for the prevention of central hypoxia and necrosis of spheroids. *Biomaterials* **33**, 8430–8441 (2012).
68. Akiyama, H., Shukunami, C., Nakamura, T. & Hiraki, Y. Differential expressions of BMP family genes during chondrogenic differentiation of mouse ATDC5 cells. *Cell Struct. Funct.* **25**, 195–204 (2000).
69. Nilsson, O. *et al.* Gradients in bone morphogenetic protein-related gene expression across the growth plate. *J. Endocrinol.* **193**, 75–84 (2007).
70. Blair, H. C. *et al.* Osteoblast Differentiation and Bone Matrix Formation In Vivo and In Vitro. *Tissue Eng. Part B. Rev.* **23**, 268 (2017).
71. Lamandé, S. R. *et al.* Modeling human skeletal development using human pluripotent stem cells. *Proc. Natl. Acad. Sci. U. S. A.* **120**, (2023).
72. Carter, M. & Shieh, J. C. Cell Culture Techniques. *Guid. to Res. Tech. Neurosci.* 281–296 (2010). doi:10.1016/B978-0-12-374849-2.00013-6
73. Mangiavini, L., Merceron, C. & Schipani, E. Analysis of Mouse Growth Plate Development. *Curr. Protoc. Mouse Biol.* **6**, 67 (2016).
74. Sebbag, E. *et al.* The world-wide burden of musculoskeletal diseases: a systematic analysis of the World Health Organization Burden of Diseases Database. *Ann. Rheum.*

Dis. **78**, 844–848 (2019).
75. BMUS: The Burden of Musculoskeletal Diseases in the United States | Prevalence, Societal and Economic Cost. Available at: https://www.boneandjointburden.org/. (Accessed: 3rd August 2023)
76. Hermann, W., Lambova, S. & Müller- Ladner, U. Current Treatment Options for Osteoarthritis. *Curr. Rheumatol. Rev.* **14**, 108–116 (2018).
77. Abramoff, B. & Caldera, F. E. Osteoarthritis: Pathology, Diagnosis, and Treatment Options. *Med. Clin. North Am.* **104**, 293–311 (2020).
78. Palepu, V., Kodigudla, M. & Goel, V. K. Biomechanics of Disc Degeneration. *Adv. Orthop.* **2012**, 1–17 (2012).
79. Schizas, C., Kulik, G. & Kosmopoulos, V. Disc degeneration: Current surgical options. *Eur. Cells Mater.* **20**, 306–315 (2010).
80. Abad, V. *et al.* The Role of the Resting Zone in Growth Plate Chondrogenesis. *Endocrinology* **143**, 1851–1857 (2002).
81. Baron, J. *et al.* Short and tall stature: A new paradigm emerges. *Nat. Rev. Endocrinol.* **11**, 736–746 (2015).
82. Jee, Y. H. & Baron, J. The Biology of Stature. *J. Pediatr.* **173**, 32 (2016).
83. Sutter, N. B., Mosher, D. S., Gray, M. M. & Ostrander, E. A. Morphometrics within dog breeds are highly reproducible and dispute Rensch's rule. *Mamm. Genome* **19**, 713 (2008).
84. Belluoccio, D. *et al.* Sorting of growth plate chondrocytes allows the isolation and characterization of cells of a defined differentiation status. *J. Bone Miner. Res.* **25**, 1267–1281 (2010).
85. Landis, W. J., Jacquet, R., Hillyer, J. & Zhang, J. Analysis of Osteopontin in Mouse Growth Plate Cartilage by Application of Laser Capture Microdissection and RT-PCR. *http://dx.doi.org/10.1080/03008200390152052* **44**, 28–32 (2009).
86. Wu, Y. X. *et al.* CD146+ skeletal stem cells from growth plate exhibit specific chondrogenic differentiation capacity in vitro. *Mol. Med. Rep.* **16**, 8019–8028 (2017).
87. James, A. W. *et al.* Isolation and characterization of canine perivascular stem/stromal cells for bone tissue engineering. *PLoS One* **12**, e0177308 (2017).
88. Tormin, A. *et al.* CD146 expression on primary nonhematopoietic bone marrow stem cells is correlated with in situ localization. *Blood* **117**, 5067–5077 (2011).
89. Espagnolle, N. *et al.* CD146 expression on mesenchymal stem cells is associated with their vascular smooth muscle commitment. *J. Cell. Mol. Med.* **18**, 104–114 (2014).
90. Fonseca, L. N. *et al.* Cell surface markers for mesenchymal stem cells related to the skeletal system: A scoping review. *Heliyon* **9**, e13464 (2023).
91. Wu, L. *et al.* Human developmental chondrogenesis as a basis for engineering chondrocytes from pluripotent stem cells. *Stem Cell Reports* **1**, 575–589 (2013).
92. De Schauwer, C., Meyer, E., Van de Walle, G. R. & Van Soom, A. Markers of stemness in equine mesenchymal stem cells: a plea for uniformity. *Theriogenology* **75**, 1431–1443 (2011).
93. Kostina, D. *et al.* Isolation of Human Osteoblast Cells Capable for Mineralization and Synthetizing Bone-Related Proteins In Vitro from Adult Bone. *Cells* **11**, (2022).
94. Schulze-Tanzil, G. Activation and dedifferentiation of chondrocytes: Implications in cartilage injury and repair. *Ann. Anat. - Anat. Anzeiger* **191**, 325–338 (2009).
95. Ghosh, S. *et al.* Dedifferentiation alters chondrocyte nuclear mechanics during in vitro culture and expansion. *Biophys. J.* **121**, 131–141 (2022).

96. Minegishi, Y., Hosokawa, K. & Tsumaki, N. Time-lapse observation of the dedifferentiation process in mouse chondrocytes using chondrocyte-specific reporters. *Osteoarthr. Cartil.* **21**, 1968–1975 (2013).
97. Huang, W., Yang, S., Shao, J. & Li, Y. P. Signaling and transcriptional regulation in osteoblast commitment and differentiation. *Front. Biosci.* **12**, 3068 (2007).
98. Kengla, C., Kidiyoor, A. & Murphy, S. V. Bioprinting Complex 3D Tissue and Organs. *Kidney Transplantation, Bioeng. Regen. Kidney Transplant. Regen. Med. Era* 957–971 (2017). doi:10.1016/B978-0-12-801734-0.00068-0
99. Skardal, A. Bioprinting Essentials of Cell and Protein Viability. *Essentials 3D Biofabrication Transl.* 1–17 (2015). doi:10.1016/B978-0-12-800972-7.00001-3
100. Campbell, D. D. & Pei, M. Surface Markers for Chondrogenic Determination: A Highlight of Synovium-Derived Stem Cells. *Cells* **1**, 1107 (2012).
101. Fan, W. *et al.* CD105 promotes chondrogenesis of synovium-derived mesenchymal stem cells through Smad2 signaling. *Biochem. Biophys. Res. Commun.* **474**, 338–344 (2016).
102. Hagmann, S. *et al.* Fluorescence activated enrichment of CD146+ cells during expansion of human bone-marrow derived mesenchymal stromal cells augments proliferation and GAG/DNA content in chondrogenic media. *BMC Musculoskelet. Disord.* **15**, (2014).
103. Watson, J. T. *et al.* CD271 as a marker for mesenchymal stem cells in bone marrow versus umbilical cord blood. *Cells. Tissues. Organs* **197**, 496–504 (2013).
104. Cicione, C., Díaz-Prado, S., Muiños-López, E., Hermida-Gómez, T. & Blanco, F. J. Molecular profile and cellular characterization of human bone marrow mesenchymal stem cells: Donor influence on chondrogenesis. *Differentiation* **80**, 155–165 (2010).
105. Dominici, M. *et al.* Minimal criteria for defining multipotent mesenchymal stromal cells. The International Society for Cellular Therapy position statement. *Cytotherapy* **8**, 315–317 (2006).
106. Lee, H. J., Choi, B. H., Min, B.-H. & Park, S. R. Changes in Surface Markers of Human Mesenchymal Stem Cells During the Chondrogenic Differentiation and Dedifferentiation Processes In Vitro. *ARTHRITIS Rheum.* **60**, 2325–2332 (2009).
107. Krešić, N. *et al.* The Expression Pattern of Surface Markers in Canine Adipose-Derived Mesenchymal Stem Cells. *Int. J. Mol. Sci.* **22**, (2021).
108. Fomby, P. *et al.* Stem cells and cell therapies in lung biology and diseases: Conference report. *Ann. Am. Thorac. Soc.* **12**, 181–204 (2010).
109. Jacquet, R., Hillyer, J. & Landis, W. J. Analysis of connective tissues by laser capture microdissection and reverse transcriptase-polymerase chain reaction. *Anal. Biochem.* **337**, 22–34 (2005).
110. Pittenger, M. F. *et al.* Multilineage potential of adult human mesenchymal stem cells. *Science (80-.).* **284**, 143–147 (1999).
111. An, C., Cheng, Y., Yuan, Q. & Li, J. IGF-1 and BMP-2 induces differentiation of adipose-derived mesenchymal stem cells into chondrocytes-like cells. *Ann. Biomed. Eng.* **38**, 1647–1654 (2010).
112. Park, K. H. & Na, K. Effect of growth factors on chondrogenic differentiation of rabbit mesenchymal cells embedded in injectable hydrogels. *J. Biosci. Bioeng.* **106**, 74–79 (2008).
113. Danišovič, Ľ., Varga, I. & Polák, Š. Growth factors and chondrogenic differentiation of mesenchymal stem cells. *Tissue Cell* **44**, 69–73 (2012).

114. Arufe, M. C., De La Fuente, A., Fuentes, I., De Toro, F. J. & Blanco, F. J. Chondrogenic potential of subpopulations of cells expressing mesenchymal stem cell markers derived from human synovial membranes. *J. Cell. Biochem.* **111**, 834–845 (2010).
115. Teunissen, M. *et al.* Growth plate expression profiling: Large and small breed dogs provide new insights in endochondral bone formation. *J. Orthop. Res.* **36**, 138–148 (2018).
116. Goldman, V. & Green, D. W. Advances in growth plate modulation for lower extremity malalignment (knock knees and bow legs). *Curr. Opin. Pediatr.* **22**, 47–53 (2010).
117. Rony, I. K. *et al.* Inducing pluripotency in vitro: Recent advances and highlights in induced pluripotent stem cells generation and pluripotency reprogramming. *Cell Prolif.* **48**, 140–156 (2015).
118. Kamakura, T. *et al.* Collagen X Is Dispensable for Hypertrophic Differentiation and Endochondral Ossification of Human iPSC-Derived Chondrocytes. *JBMR Plus* **7**, e10737 (2023).
119. Zhang, M. *et al.* Recapitulation of cartilage/bone formation using iPSCs via biomimetic 3D rotary culture approach for developmental engineering. *Biomaterials* **260**, 120334 (2020).
120. Omole, A. E. & Fakoya, A. O. J. Ten years of progress and promise of induced pluripotent stem cells: Historical origins, characteristics, mechanisms, limitations, and potential applications. *PeerJ* **2018**, e4370 (2018).
121. Huo, J. *et al.* Evaluation of Batch Variations in Induced Pluripotent Stem Cell-Derived Human Cardiomyocytes from 2 Major Suppliers. *Toxicol. Sci.* **156**, 25–38 (2017).

Supplementary

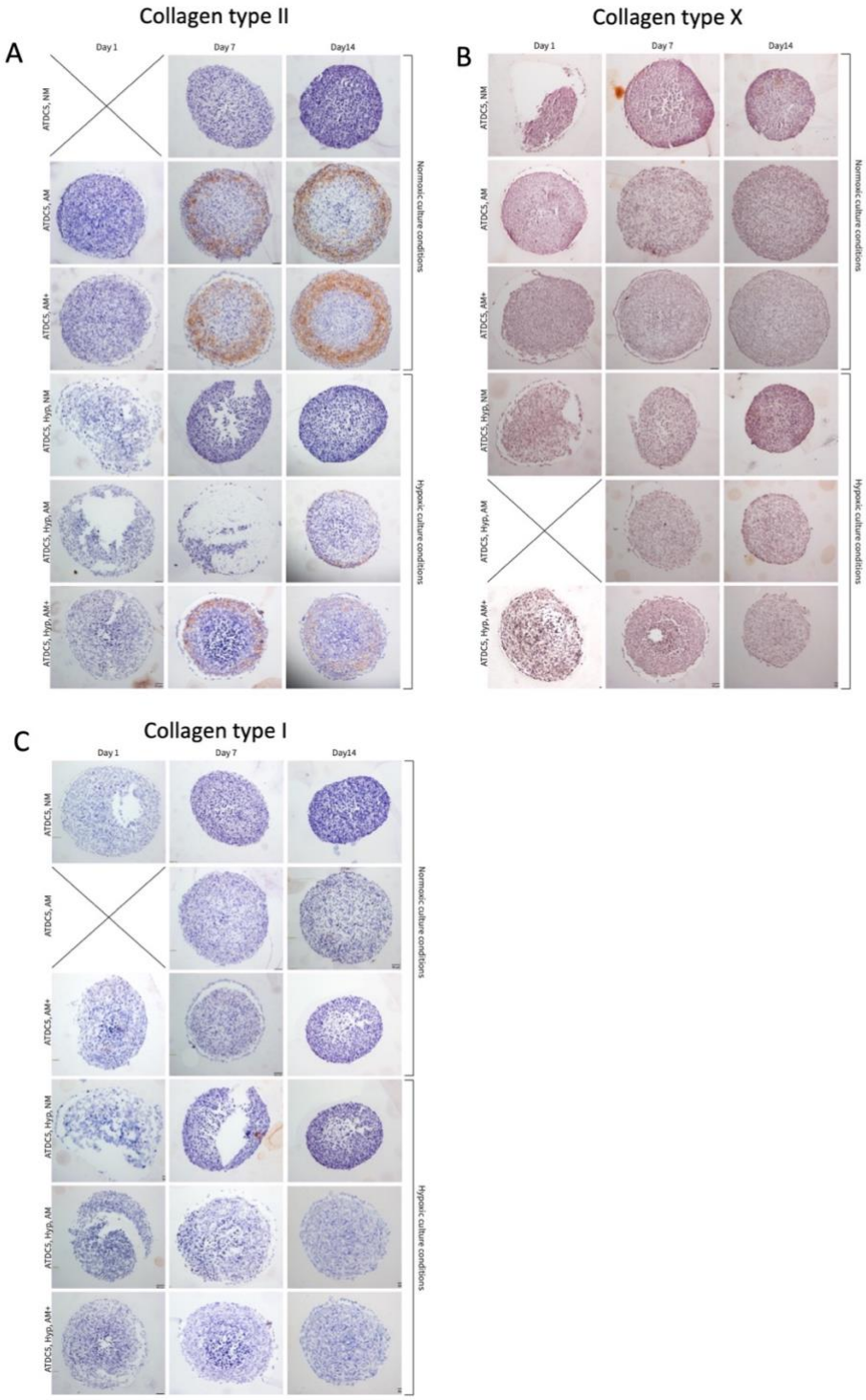

Figure S1: Collagen type I, type II, and type X production by ATDC5 micro-aggregates (35.000 cells) cultured with just ITS (NM), full chondrogenic culture medium supplemented with TGF-β (AM) and full chondrogenic differentiation medium supplemented with TGF-β and FBS (AM+) (Left Y-axis). Micro-aggregates were cultured in two conditions (right Y-axis). Culture period is shown on the X-axis. Immunohistochemical qualification of A) collagen type II, B) collagen type X and C) collagen type I. Crosses indicate missing data.

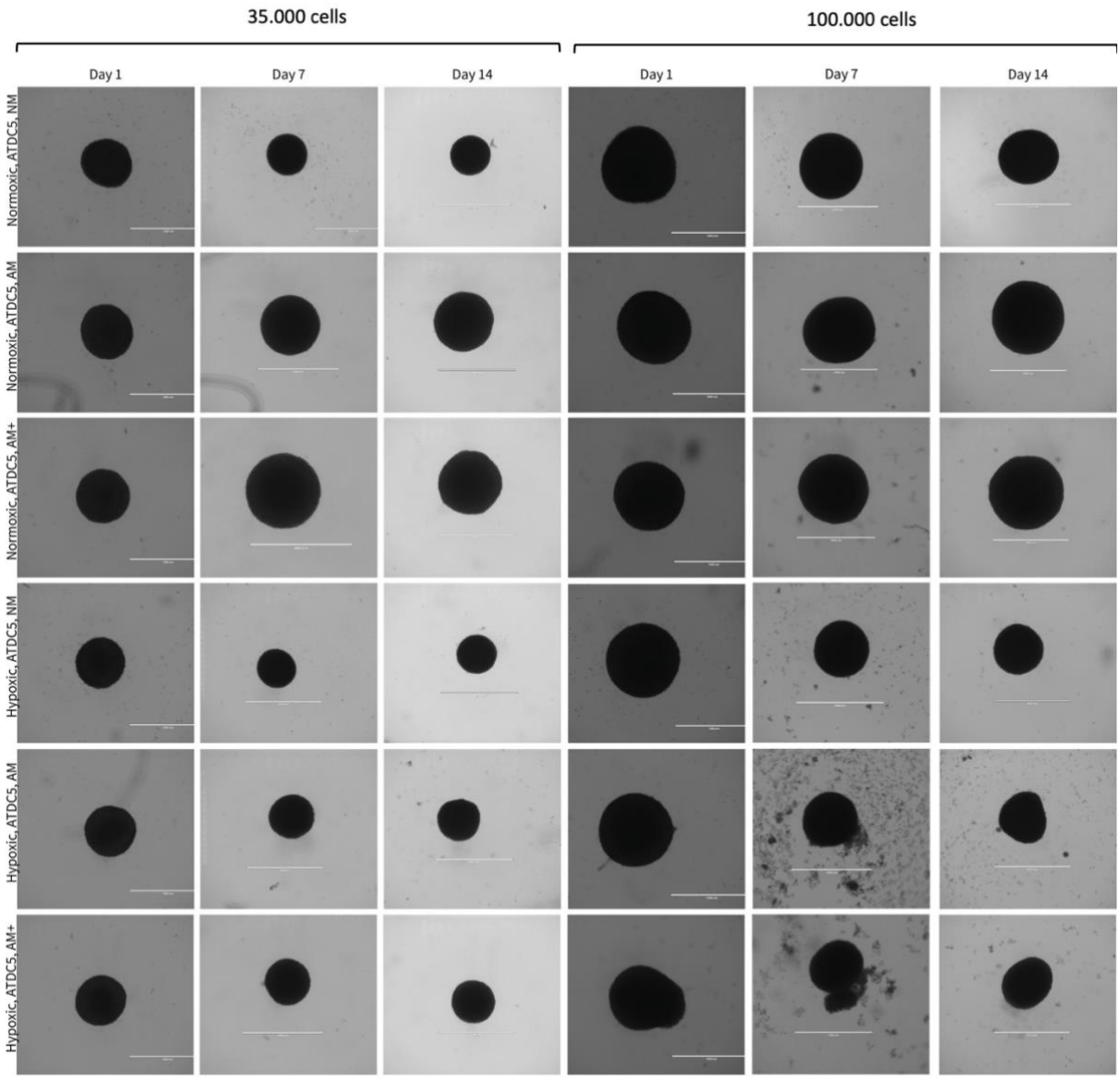

Figure S2: overview of pellet growth for the first ATDC5 3D culture experiment. Culture conditions are noted on the Y-axis and culture time is noted on the X-axis. A distinction can be made between 35.000 cells and 100.000 cells. white scale bar represents 1000 µm.

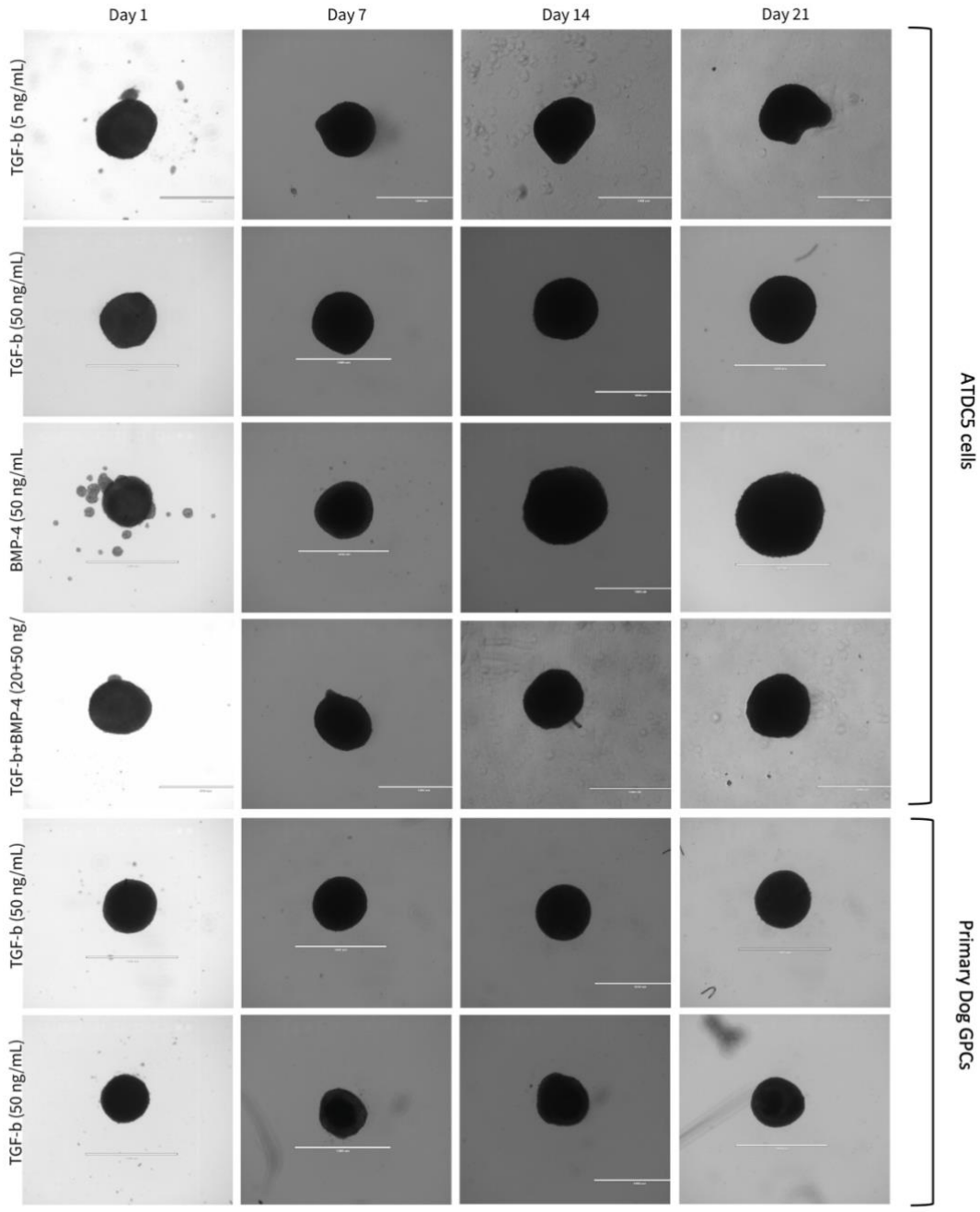

Figure S3: overview of pellet growth for the second 3D culture experiment. Culture conditions are noted on the Y-axis and culture time is noted on the X-axis. A distinction can be made between ATDC5 cells and primary dog GPCs. white scale bar represents 1000 µm.

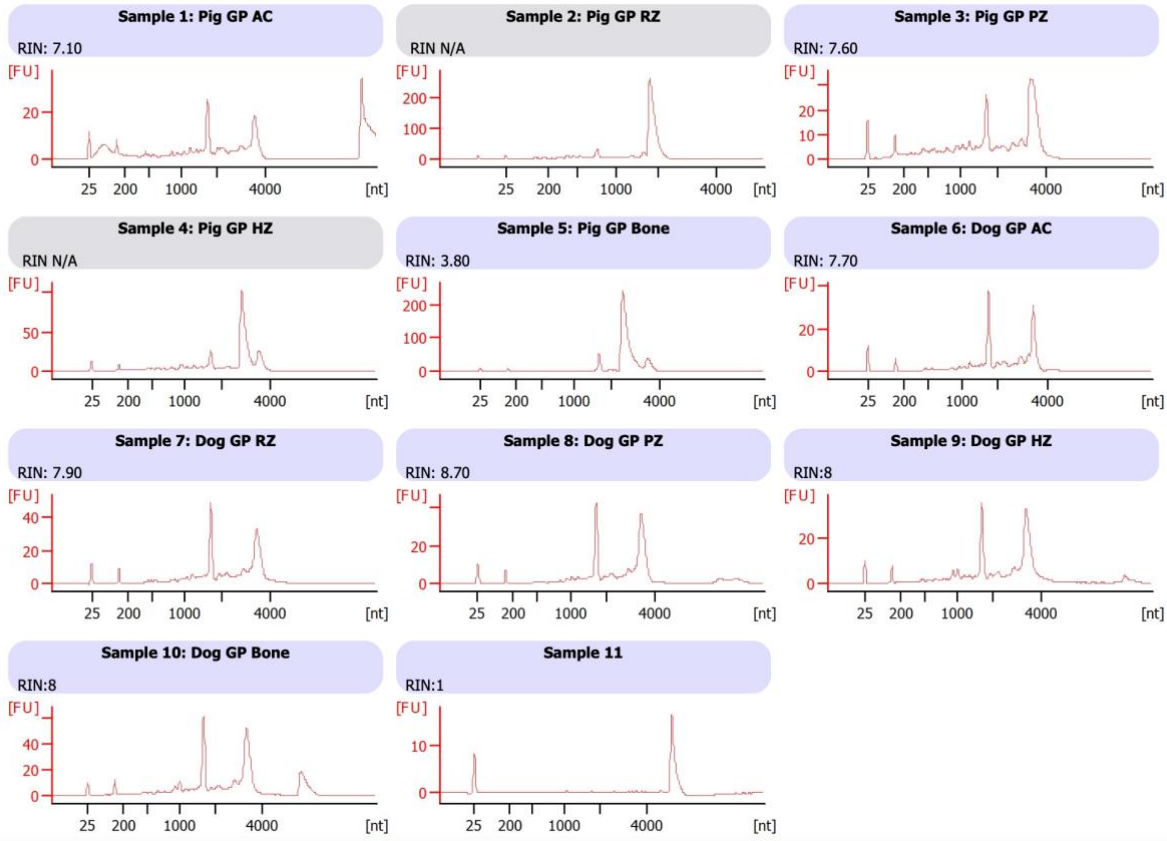

Figure S4: Analysis of RNA integrity after tissue decalcification and cryosectioning. RNA integrity is displayed by the RIN value.